Corrosion initiation mechanisms and service life estimation of concrete systems with fusion-bonded-epoxy (FBE) coated steel exposed to chlorides

Deepak K. Kamde and Radhakrishna G. Pillai

Department of Civil Engineering, Indian Institute of Technology Madras, Chennai, India

Cite this article as: Deepak K. Kamde and Radhakrishna G. Pillai (2021) "Corrosion initiation mechanisms and prediction of the service life of concrete systems with fusion-bonded-epoxy (FBE) coated steel rebars and exposed to chlorides," Construction and Building Materials, Elsevier, Vol. 277, 122314, https://doi.org/10.1016/j.conbuildmat.2021.122314

ABSTRACT

This paper evaluates the suitability of various techniques such as half-cell potential, macrocell corrosion, linear polarization resistance, and electrochemical impedance spectroscopy (EIS) to detect corrosion initiation of fusion-bonded-epoxy (FBE) coated steel rebars in concrete. It was found that EIS is the best technique for this purpose. Then, a new test method (named as "cs-ACT" test) using EIS is developed to detect the initiation of corrosion and determine chloride threshold at the coating-steel interface, which was not a practice in the literature. Also, the reduction in the resistance of the FBE coating was monitored and a a 4-stage degradation process and corrosion initiation process are identified and discussed using SEM, EDAX, and statistical analysis of the change in the polarization resistance of steel (from repeated EIS tests - Nyquist/Bode plots). Then, a new method that uses the properties of epoxy coating, steel-coating interface, and concrete cover to estimate the service life of reinforced concrete systems with FBE coated rebars is demonstrated. Modifications to the existing specifications to achieve target service life are also proposed.

Keywords: Fusion-bonded-epoxy, coated rebar, steel, chlorides, corrosion initiation, thickness, degradation, concrete, service life

HIGHLIGHTS

i. Conventional test methods failed to detect the initiation of corrosion of FBE coated steel rebars
ii. An EIS-based methodology is proposed to detect the initiation of corrosion of FBE coated steel rebars in concrete
iii. A methodology to determine the chloride threshold of FBE coated steel rebar is proposed
iv. Degradation mechanism of FBE coating due to exposure to moist, alkaline environment with chlorides is proposed
v. A new framework for the estimation of service life of RC structures with FBE coated steel rebars is proposed and demonstrated

LIST OF SYMBOLS AND ABBREVIATIONS

%bwob	:	% by weight of binder
Cl_{th}	:	Critical chloride threshold of steel-coating interface
CPE_C	:	Capacitance of the coating
$CPE_{C\text{-}S}$	:	Capacitance of the coating-steel interface
D_{cl}	:	Chloride diffusion coefficient of concrete
EEC	:	Equivalent Electrical Circuit
FBE	:	Fusion-Bonded-Epoxy
FBEC-ND	:	FBE coated steel rebars in as-received condition with no damage/degradation
FBEC-SD	:	FBE coated steel rebars with scratch damage to coating
m	:	Decay constant
RC	:	Reinforced concrete
R_C	:	Resistance of the coating
$R_{P,\ C\text{-}S}$	:	Polarization resistance of the coating-steel interface
R_S	:	Resistance offered by the electrolyte solution
S-C	:	Steel-Coating interface
t_{SL}	:	Time to corrosion initiation
$t_{coating}$	:	Coating thickness
x	:	Depth from the exposed surface of concrete
x_{epoxy}	:	Depth from the exposed surface of coating

1 INTRODUCTION

Many reinforced concrete (RC) structures are desired to last many decades. In anticipation of such a long life, RC structures in coastal regions are/were built with coated steel rebars. Fusion-bonded-epoxy (FBE) coated steel rebar is one of the most widely used coated steel rebars in the construction industry. In general, FBE coating protects the underlying steel by (i) providing a physical barrier from the surrounding environment, (ii) limiting the formation of anodic and cathodic sites, and (iii) restricting the ionic conduction between anodic and cathodic sites at steel surface [1]. ASTM A775 is a widely used standard specifying the properties of FBE coated steel rebars. However, meeting these requirements at construction sites is challenging. The FBE coating has poor abrasion resistance and gets damaged due to inadequate handling such as bending and dragging of rebars at construction sites – a common scenario in many construction sites.

Figure 1(a) shows that the rebars are bent using mettalic lever, which can result in the damaged coating at the bent location and at the place where metallic lever is held. Figure 1(b) shows that the coating on steel rebars are damaged due to dragging of the FBE coated steel at the construction sites. Therefore, the listed three protection mechanisms may not be valid. Many infrastructure with FBE coated steel rebars have shown distress due to corrosion within 30 years of service life [2–10]. Therefore, worldwide, many parts in the USA, Europe, Canada, etc., have either banned or recommended not to use the FBE coated steel rebars (see Table 1). On the other hand, many laboratory studies report the good performance of coated steel rebars [11–16]. This difference in opinion between lab and field studies can be due to (i) the difference in the quality of coated steel rebars used at sites and at laboratories and (ii) the use of test methods that are not adequate to assess the RC systems with FBE coated steel rebars (see Table 2). Also, the existing service life models, which are meant for RC systems with uncoated steel rebars, do not consider the diffusion of chloride through the coating and true

chloride threshold of coated steel. Therefore, these service life estimation models may not be adequate for RC systems with coated steel rebars. This paper investigates the suitability of existing test methods in detecting the initiation of corrosion in RC systems with FBE coated steel rebars. Then, a methodology based on a suitable technique is proposed to detect the initiation of corrosion in RC systems with FBE coated steel rebars. Also, the framework for the estimation of service life is proposed. Then, the effects of coating thickness and damage to coating on the service life of RC systems are quantified.

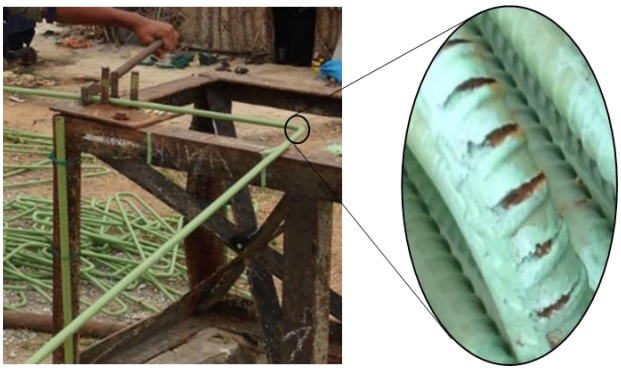

(a) Bending of FBE coated steel rebars using metallic levers at construction sites – resulting in damage/cracking of coating

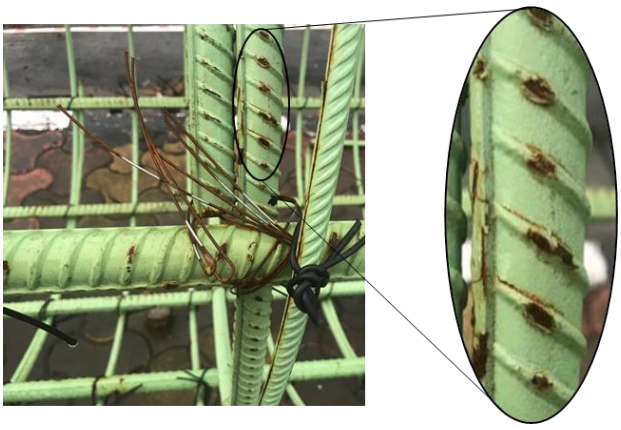

(b) Scratch damage to coating due to dragging of rebars at construction sites

Figure 1 Photographs of typical damage to FBE coating due to inadequate practices at construction sites

Table 1 Details on the recommendations on the use of FBE coated steel

Country; Reference	Recommendation on the use of FBE coated steel rebars
Florida, USA; [17]	In 1979, banned to be used in bridges and large infrastructure
Florida, USA	In 1988, banned from all the construction projects
Oregon, USA; [3]	In 1989, (recommended to stop using FBE coated steel rebars
Quebec, Canada; [8]	In 2000, the further use of FBE coated steel rebar was not recommended
Ontario, Canada; [18]	In 2000, The use of FBE coated steel steel rebar was not recommended based on technical reasons and life-cycle cost analysis
Virginia, USA; [4]	In 2000, recommended to stop using FBE coated steel rebar

Table 2 Reported techniques used for assessing the performance of FBE coated steel rebar

Test method/technique	Key finding on the performance of FBE coated steel rebars	Reference
HCP, MC current, and VOB	Based on corrosion measurements recorded, FBE coated steel showed better performance than uncoated steels.	[11,13,14,16,19–21]
LPR	The corrosion rate of undamaged FBE coated steel rebars was found significantly low.	[22]
EIS and VOB	The damaged coating can lead to localized/pitting corrosion of steel at damaged locations.	[23]
	FBE coated steel rebars can provide an additional five years of service life as compared to uncoated steel rebars.	[8,24]
LPR and Ground Penetrating radars	Showed limited success in assessment of corrosion in concrete systems	[25]

[Note: HCP: half-cell potential, MC: macrocell corrosion, VOB: visual observation, LPR: linear polarisation resistance, EIS: electrochemical impedance spectroscopy].

1.1.1 Half-cell potential (HCP)

HCP mapping is one of the most widely used methodologies for the assessment of RC systems. ASTM C876 (1999) guides to evaluate the probability of corrosion activities for uncoated steel rebar surface using HCP measurements on the surface of concrete [26]. For HCP measurements, one end of the voltmeter is electrically connected to the steel rebars and the other end is connected to the reference electrode. The reference electrode is placed on the saturated concrete surface, where the steel rebar is electrically connected to the voltmeter. HCP measurements of RC systems with uncoated steel rebars provide probabilistic information on active/inactive corrosion. However, it does not give information of the rate of corrosion [27]. In addition. HCP measurements of uncoated steel in concrete is challenging due to the high resistivity of concrete, varying relative humidity in concrete, etc. [28,29]. The large ohmic drop across coating can be an additional challenge for HCP measurements of RC systems with coated steels. Therefore, the use of existing methodology can lead to erroneous interpretation of the measurements of the corrosion of underlying steel in coated steel rebars [30]. However, many literature report the performance of FBE coated steel rebars using HCP (see Table 1). Therefore, the suitability of HPC in detecting the initiation of corrosion is also assessed in this paper.

1.1.2 Macrocell corrosion (MC) current

MC current is another test method for determining the effect of chemical admixtures on corrosion of embedded uncoated steel rebars using macrocell specimens [31]. The macrocell specimens have well separated anodic and cathodic rebars. The rebars are electrically connected by using a resistor. Then, the macrocell current is measured by measuring the potential difference between the anode and cathodes. When corrosion initiate, the macrocell current is expected to be significantly higher than when no corrosion activity take place. The detection of the initiation of corrosion using macrocell specimens was reported to be not

possible when the resistivity of concrete is high [32,33]. Similarly, the ionic resistance offered by FBE coating is significantly high [20,34]. Therefore, corrosion cells may not form between top and bottom steel rebars of macrocell specimens without the participation of the bottom rebar [19]. Therefore, assessment using MC current may not be suitable for the assessment of concrete systems with FBE coated steel rebars. However, many literatures report the performance of FBE coated steel rebars using macrocell specimens [11,35], which can misguide the construction decision-makers and stakeholders.

1.1.3 Linear polarization resistance (LPR)

Test methods based on LPR techniques are widely used to measure the rate of corrosion of uncoated rebars in concrete systems. For LPR measurements, the open circuit potential of test specimen is measured and is polarized to a small range (usually, less than ±20 mV). The resultant current is measured. The slope of the curve between potential applied and measured current at the free corrosion potential represents the resistance to polarization, which can be used to measure the rate of corrosion [36]. Literature report that the LPR measurements can capture the corrosion activity of the uncoated metal surface, where resistance offered by solution/electrolyte is less than 37 kΩ.cm [37,38]. The resistance of a good quality FBE coating (R_C) is approximately 1000 kΩ.cm [20]. The high R_C can result in a significantly high ohmic drop across the FBE coating, which can influence the measurements of resistance to polarization (R_P) using LPR [37]. In addition to large ohmic drop, non-homogeneous distribution of the absorbed moisture in the coating can lead to erroneous quantifications of current interruption [39]. Also, the R_P measured using the LPR technique gives the bulk response of anything between the electrolyte and steel surface [40]. Therefore, with existing test methods, it may not be possible to capture the changes in R_P due to the initiation of corrosion.

1.1.4 Electrochemical impedance spectroscopy (EIS)

The principle of EIS is to apply an AC signal of small amplitude (say, 10 mV) to the working electrode (here, uncoated and FBE coated steel rebar) embedded in electrolyte such as concrete. The initial disturbance is small potential applied (ΔE) under steady state conditions, and the response from the electrode (i.e., sinusoidal current (ΔI)) with a phase difference (Φ) from the applied small voltage. Therefore, the impedance (Z) is the measures the relationship between ΔE and ΔI. Test methods based on EIS have been used to assess the coated metal structures. A few literature report that EIS technique can overcome challenges such as high resistivity of electrolyte, nonuniform distribution of moisture in the coating, and considerable variation of R_P [39,41,42]. Assessment using the EIS technique can also produce reliable data by limiting the error of each component using the equivalent electrical circuit (EEC) [43]. However, many of the published articles focus on the assessment of coated steels exposed to the aqueous solution, which may not simulate the coated steel rebars embedded in concrete systems. Sagues and Zayed (1991) proposed one of the first methods based on EIS to measure the corrosion rate of FBE coated steel rebars in concrete with damaged coating [44]. However, this method may not be directly applicable to assess RC systems with FBE coated steel rebars with undamaged coatings. A few literature report that the EIS can be one of the techniques capable of assessing coated steel rebars embedded in cementitious systems [10,23,51,30,44–50], which is adopted in this study. However, the authors could not find literature on methodologies to detect the initiation of corrosion in RC systems with FBE coated steel rebars. Therefore, this paper investigates the electrochemical response of FBE coated steel rebars with and without damage to the coating and proposes a generalized EEC to detect the initiation of corrosion.

1.2 Parameters to estimate the service life of RC systems with FBE coated rebars

The service life of the RC system is defined as the time during which the structure can safely meet the user requirements. It is the summation of the corrosion initiation and corrosion propagation phase [52]. The initiation phase is the time required for chlorides to diffuse through the concrete and reach a sufficient amount on the steel surface to initiate the corrosion. The initiation phase depends on factors such as surface chloride concentration, diffusion coefficient, decay constant, and chloride threshold of steel-binder interface [53–55]. The minimum chloride concentration needed to initiate the corrosion is known as chloride threshold (Cl_{th}) [56]. The propagation phase depends on many factors such as chloride concentration at rebar level, concrete resistivity, rate of corrosion, oxygen and moisture condition at the rebar level [52,57]. Generally, as a conservative approach, the initiation phase is considered to the service life.

In the case of FBE coated steel rebars, chlorides have to diffuse through the cover concrete then through the epoxy coating to reach the steel surface. Therefore, in addition to the parameters discussed for RC systems with uncoated steel rebars, the chloride diffusion coefficient of FBE coating needs to be considered, which is not considered in the reported literature. A good quality epoxy coating with a significantly low chloride diffusion coefficient reduce the rate of transport of chlorides through the coating, and may have significantly high service life [20,58]. It was also reported that the even if the quality of coating is good, the moisture and chlorides can diffuse into epoxy coating [59]. It was reported that the chloride concentration on the coating surface at the time of initiation of corrosion was about 2.5 %by weight of binder [21,24,60]. However, these chloride concentrations do not participate in the corrosion process and are not the Cl_{th}. Therefore, for FBE coated steel without damage to coating, chlorides at the steel surface (i.e., beneath the coating) required to initiate the corrosion are known as Cl_{th} [61].

For the case of FBE coating with damaged coating, the chlorides in the mortar/concrete are in contact with steel surface at damage level. Therefore, the chlorides at steel-mortar interface, which required to initiate the corrosion, is the Cl_{th}. The Cl_{th} depends on the microclimate (such as crevice at defects, pH level, moisture and oxygen level) at the steel-coating interface [62]. Kessler et al. reported that the defect size could influence the Cl_{th} [19]. Kamde and Pillai reported that the microcracks in concrete could reduce the Cl_{th} [58]. Therefore, Cl_{th} should be determined on the coated steel rebars reflecting the in-service conditions of coated steel rebars at sites. Then, the time to initiation of corrosion for RC systems with FBE coated steel rebars should be estimated by considering the Cl_{th} and $D_{Cl,\ concrete}$. The Cl_{th} depends on the microclimate (such as crevice at defects, pH level, moisture and oxygen level) at the steel-coating interface [19,62]. Therefore, Cl_{th} should be determined on the coated steel rebars reflecting the in-service conditions of coated steel rebars at sites. Then, the time to initiation of corrosion for RC systems with FBE coated steel rebars should be estimated by considering the Cl_{th} and $D_{Cl,\ concrete}$. This paper presents frameworks to evaluate these critical parameters and to estimate the service life of RC systems with FBE coated steel rebars.

2 RESEARCH SIGNIFICANCE

Detecting initiation of corrosion is an important aspect to quantify the chloride threshold of FBE coated steel rebars. Many practitioners use conventional test methods based on HCP, MC, and LPR to detect the initiation of corrosion in RC systems with FBE coated steel rebars. The results presented in this paper indicate that these test methods could not detect the initiation of corrosion in such systems. The proposed test methods based on EIS will enable practitioners to detect the initiation of corrosion in concrete systems with FBE coated steel rebars. The framework will enable engineers to estimate the residual corrosion-free service life, and plan for the repair of such RC systems.

3 EXPERIMENTAL METHODS

This paper is presented in two phases. Phase 1 involves the experimental study on the assessment of the suitability of conventional test methods in detecting the initiation of corrosion in FBE coated steel rebars. Then, a methodology to detect the initiation of corrosion in RC systems with FBE coated steel rebars embedded in cementitious systems is proposed. In Phase 2, a framework is proposed to determine the diffusion coefficient of coating, chloride threshold of FBE coated steel rebars, and estimate the service life of RC system with FBE coated steel rebars. Then, the effect of coating thickness and damage to coating on the service life of RC systems is quantified. The FBE coated steel rebars used in Phase 1 and Phase 2 were found to have a maximum of two holidays per meter length of steel rebars. The coating thickness of the FBE coating was measured using the coating thickness gauge. The coating thickness was found to be varying throughout the length. Therefore, the FBE coated steel with a coating thickness of 175 µm to 420 µm was selected for Phase 1 and Phase 2, which is closest to the requirements as per ASTM A775.

In these studies, the mortar was used (instead of concrete) because chloride threshold (Cl_{th}) is a steel-coating and steel-binder interface property for FBE coated steel rebars and uncoated steel rebars, respectively [62,63]. Cl_{th} depends on the local characteristics (or microclimate) of the steel-coating and steel-binder interface [59]. The microclimate at the steel-coating-concrete interface can change due to many factors, including the presence of aggregates. However, the influence of the presence of inert aggregates on Cl_{th} is due to the indirect effect of the change in the microclimate of steel-coating-concrete interface. To avoid nonuniformities in the physical microclimate at the steel-coating and steel-binder interface, mortar was used to prepare the macrocell and lollipop specimens. Also, the use of mortar could help to reduce the test duration (fast and uniform transport of chloride) and the size of the specimens

3.1 Phase 1: Evaluation of conventional test methods

3.1.1 Evaluation of HCP and MC current

To evaluate the suitability of HCP (ASTM C876) and MC (ASTM G109), macrocell specimens similar to that prescribed in ASTM G109 were used.

3.1.1.1 Specimen preparation

Figure 2 shows the photographs of the steel rebars used in this study. Figure 3(a) shows the photograph and schematic of macrocell specimens (200 × 75 × 75) mm [(7.87 × 2.95 × 2.95) in.] prepared with the following reinforcement (i) uncoated, (ii) FBE coated steel rebars with no intentional damage (FBEC-ND), and (iii) FBE coated steel rebars with scratch damage to coating (FBEC-SD) (see Figure 2). The rebars are placed such that the top rebar is the anode and two bottom rebars act as cathodes. The anode-to-cathode ratio of all the specimens was maintained to 0.5, as suggested in ASTM G109 [31]. For the preparation of macrocell specimens, 15 uncoated steel rebars and 30 FBE coated steel rebars of 8 mm diameter were cut to the length of 200 mm (7.86 in.). To simulate the damaged coated steel rebars at the construction sites, the coating on 15 FBE coated steel rebars were scratched off using emery paper on the rib surfaces at the central 50 mm (1.96 in.) length. The coating on about 7 to 9 ribs was scratched off on each coated steel rebar. A total of maximum 0.6% of the total surface area of the coating was damaged, and these specimens were named FBEC-SD. Figure 2(c) shows the FBE coated steel rebar surface with scratched coating. 25 mm (0.98 in.) long region on both ends of all the steels were covered with electroplaters tape. This region was further covered with a heat-shrink tube to avoid the entry of moisture, oxygen, or chlorides (see Figure 3). The covering with electroplater tape and heat-shrink tube ensured that no crevice corrosion takes place at the ends of the steel specimens, which was later verified by visual inspection.

(a) Uncoated steel rebar

(b) FBE coated steel with no damage

(c) FBE coated steel with scratch damage to coating

Figure 2 Photographs of typical rebars used to prepare macrocell corrosion and lollipop specimens

After positioning of the prepared rebars in the steel moulds, the mortar was placed in the moulds to cast the macrocell specimens. The mortar with cement:sand:water/binder of 1:2.75:0.5 was used. Macrocell specimens were cast and cured in steel moulds for one day. Then, moist cured for another 27 days. Thereafter, the specimens were stored in the laboratory environment (27 ± 5 °C and 65 ± 5 % relative humidity) for the remaining exposure and testing period. The top and bottom rebars were electrically connected using 100 Ω resistor (see Figure 3). Silicone sealant was applied on the side faces of the reservoir to enable one-dimensional chloride transport through mortar cover towards the embedded steel rebar. The same specimens were used for the assessment using MC current.

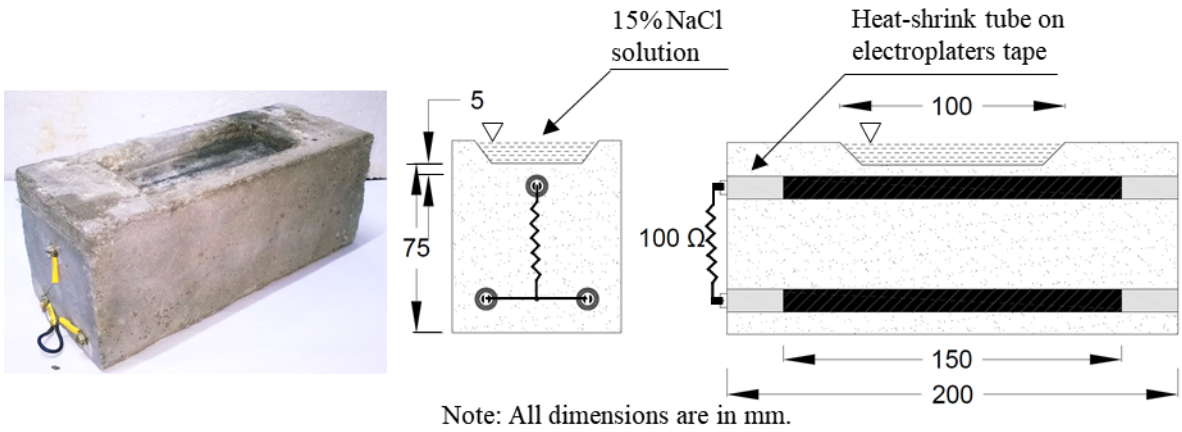

Figure 3 Macrocell corrosion test specimen [64]

3.1.1.2 Chloride exposure and electrochemical measurements

The specimens were subjected to the cyclic two days wet - five days dry exposure using simulated pore solution with 15% sodium chloride solution. At the end of each wet regime, the corrosion potentials of top rebars were measured using a Saturated Calomel Electrode (SCE), and potential differences between the top and the bottom rebars were recorded across the 100 Ω resistor. Then, MC currents were measured at the end of each wet cycle, and the cumulative charge was calculated by the trapezoidal rule. As per ASTM G109, when total corrosion was equal to or greater than 150 C, the specimens were defined to exhibit initiation of corrosion.

3.1.2 Evaluation of LPR and EIS tests using lollipop specimens

To evaluate the suitability of LPR and EIS techniques, lollipop specimens with single rebars were used.

3.1.2.1 Specimen preparation

To evaluate the suitability of LPR and EIS tests, lollipop specimens with the following steel rebars were cast: (i) uncoated steels and (ii) FBE coated steel rebars. Figure 4 shows the schematic and photograph of the lollipop specimens. To prepare the lollipop specimens, five uncoated and 15 FBE coated steel rebars of 8 mm (0.31 in.) diameter were cut to 110 mm (4.33

in.) length. Then, one end of all the steel was drilled with a 3.4 mm (0.13 in.)diameter hole, and a threaded stainless-steel rod was fastened to make the electrical connections for electrochemical tests. The stainless steel was connected to the steel rebar as the electrical connections can not be made directly to the FBE coated steel rebar due to high electrical resistance of the FBE coating. The uncoated steel pieces were cleaned and degreased using ethanol and ultrasonic cleaner, and FBE coated steels were degreased using ethanol. Then, 5 mm long portion at the end of the coated and uncoated steel rebar was covered with the heat-shrink tube. The heat-shrink tube was extended to about 5 mm (0.19 in.) to cover the threaded stainless steel. If any gap was observed between the threaded stainless-steel rod and heat-shrink tube, it was filled with low viscous epoxy to avoid entry of moisture or chlorides. The prepared steel pieces were placed in 110 mm (4.33 in.) long cylindrical molds and centered using the plastic cap with a hole in the center. Mortar with water:binder:sand ratio of 0.5:1:2.75 was placed in moulds to achieve a cover of about 10 mm (0.39 in.). Then, the specimens were cured in plastic molds for one day in the laboratory environment (25 ± 2 C and 65 ± 5% relative humidity). To restrict the exposure to center, except 50 mm (1.96 in.) mortar at the center of sp ecimens, was covered with three layers of epoxy (see Figure 4). Each layer of epoxy was cured for two to three hours, as per the manufacturer's guidelines. After curing of epoxy coats, lollipop specimens were cured in the fog room (25 ± 2 C and > 95% relative humidity) for 27 days. Then, specimens are ready to expose to chloride solution and testing.

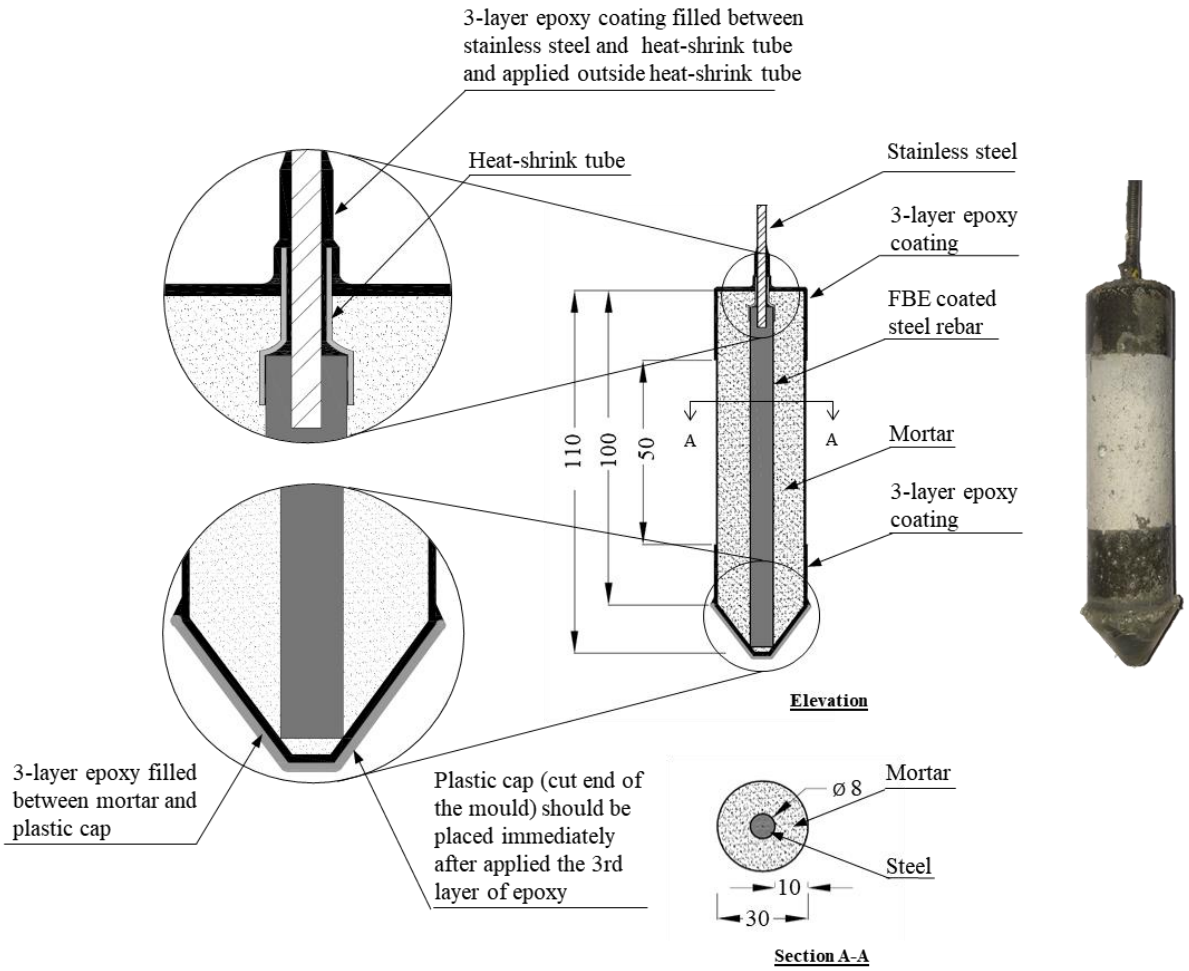

Figure 4 Schematic of the lollipop test specimen used for LPR and EIS test [64]

3.1.2.2 Exposure to chlorides and electrochemical measurements

Figure 5 shows the schematic and photograph of a three-electrode system used for LPR and EIS test. The embedded steel rebar was the working electrode, nickel-chromium mesh placed circumferentially to the lollipop specimen was the counter electrode (not shown in photograph); and SCE was the reference electrode. The simulated concrete pore solution (0.03% $Ca(OH)_2$ + 2.23% KOH + 1.04% NaOH + 96.6% of distilled water) contaminated with 3.5% NaCl was used as the immersion solution. LPR tests were performed after every wet period over a scan range of ± 15 mV with respect to the HCP at a scan rate of 0.05 mV/s. The LPR curves were obtained at the end of every wet period, and the resistance to polarisation (R_p) was determined.

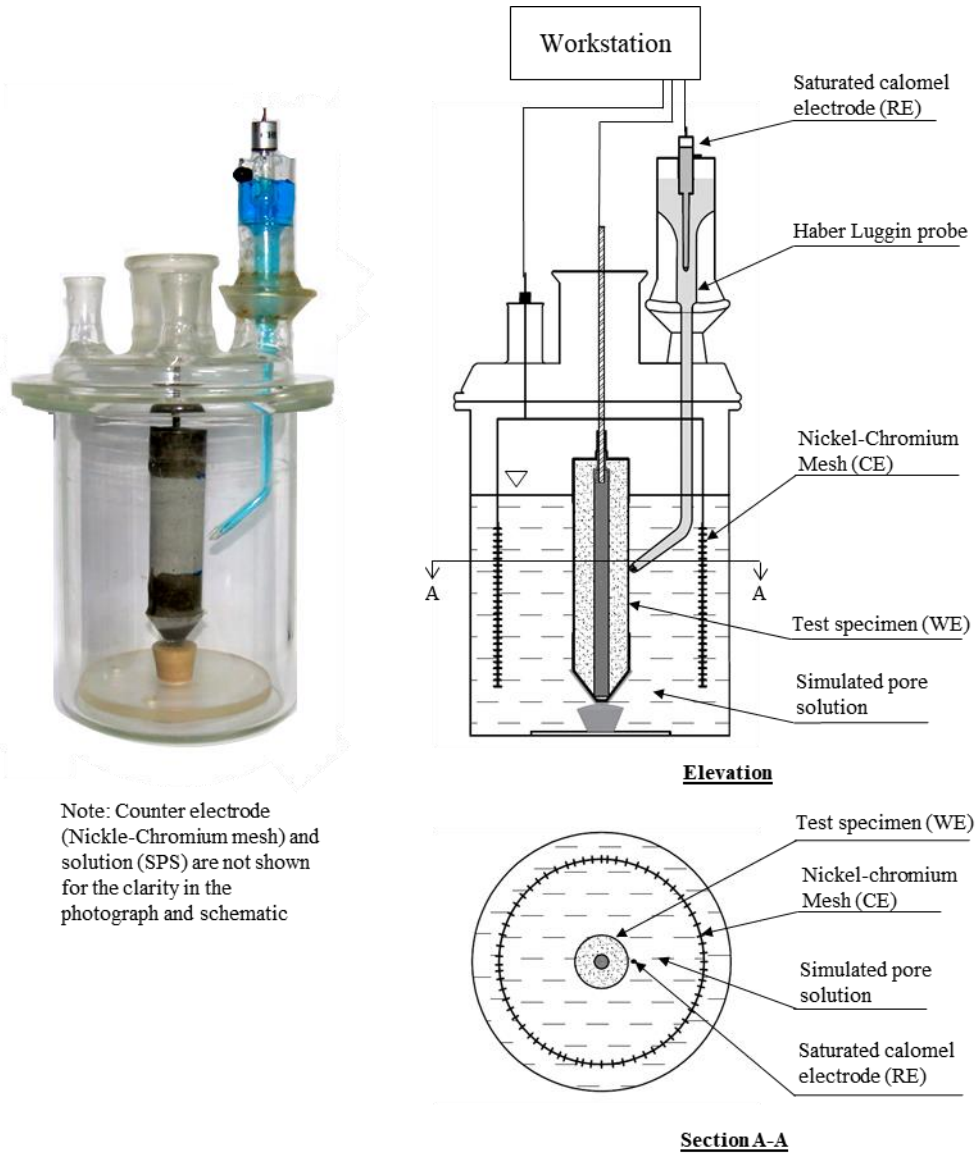

Figure 5 Photograph and schematic of three-electrode corrosion cell test setup for LPR and EIS test [64]

For the EIS study, the same corrosion cell setup was used with following input parameters: AC potential amplitude of ± 10 mV, a frequency ranges from 10^6 Hz to 0.01 Hz, the DC potential was maintained at HCP, and 10 data points per decades were collected. The signal response was analyzed, and resistances offered by each layer (mortar, coating, steel-coating interface) were quantified using the proposed EEC, which is discussed later. Then, resistance offered by the steel-coating interface ($R_{P, S-C}$) were monitored with respect to the exposure time. When five consecutive values of $1/ R_{P, S-C}$ lie within a boundary of $\mu \pm 1.3\sigma$, the system was considered to have stabilized (μ - mean; σ - standard deviation). Following this

stable state, if two future readings lie above (μ ± 3σ), corrosion is said to have been initiated [37,65]. A similar approach was adopted for assessing the initiation of corrosion using a test method based on the LPR technique.

3.2 Phase 2: Parameters to estimate the service lives of RC systems

To estimate the service life of RC system with FBE coated steel rebars, the following material properties were determined using various test methods: chloride diffusion coefficient of concrete (D_{cl}), chloride diffusion coefficient of coating ($D_{cl,\ coating}$), chloride threshold of FBE coated steel rebars (Cl_{th}), surface chloride concentration of concrete (C_s), time to build surface chloride concentration, and decay constant (m). The D_{cl}, C_s, and m were determined from field inspection of a 6-year old bridge structure and their details are presented by Kamde and Pillai [63]. $D_{cl,\ coating}$ and Cl_{th} were determined using the test methods described next.

3.2.1 Chloride diffusion coefficient of FBE coating

The chloride from the exposure environment diffuse through concrete and reach the coating surface. Due to the concentration gradient of chlorides at the coating and steel surface, chlorides start to diffuse in the coating [66]. It is assumed that the diffusion of chlorides follows Fick's second law of diffusion as shown in Equation 1.

$$Cl(x_{epoxy}, t) = Cl_{C-M} - \left(CL_{C-M} - C_{i,coating}\right) \times erf\left(\frac{x_{epoxy}}{\sqrt{4 \times D_{cl,coating} \times t}}\right) \quad (1)$$

Where, $Cl(x_{epoxy}, t)$ is the chloride concentration at the depth 'x_{epoxy}' at time 't' in the epoxy coating. $Cl_{C\text{-}M}$ is the chloride concentration at the coating-mortar interface, $C_{i,\ coating}$ is the initial chloride concentration in the FBE coating, and $D_{cl,\ coating}$ is the chloride diffusion coefficient of FBE coating, which is considered to be constant throughout the service life.

To determine the $D_{cl,\ coating}$, the coated steels are extracted from lollipop specimens after the initiation of corrosion was detected, which is discussed later. The coated steel rebars were cut to half of the cross-section, and the remaining half of the cross-section of the steel was

fractured by bending it. The half cross-section was fractured to avoid the cross-contamination of chlorides and rust products across the coating cross-section. The chloride concentrations at various depth of coating at the fractured plane were obtained using the Energy-dispersive X-ray (EDX) technique. Figure 6 shows the micrograph of the cross-section of FBE coating and representative locations to detect the chloride concentrations at various depths of FBE coating. Then, EDX responses were obtained from the fractured coating cross-sections. Adopting this methodology, three chloride profiles from 15 fractured and peeled-off coating samples from the five coated steels extracted from the lollipop specimens after the initiation of corrosion were obtained. These chloride profiles and Fick's second law of diffusion (Equation 1) was used to determine the $D_{cl,\ coating}$. Here, $D_{cl,\ coating}$ was assumed to be constant throughout the service life. Further research is required to quantify the decay constant of the FBE epoxy coating.

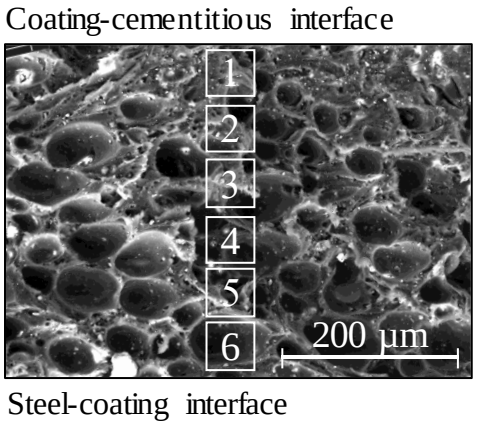

Figure 6 Framework to determine the diffusion coefficient of FBE coating

3.2.2 Chloride threshold of FBE coated steels

To evaluate the effect of damage to the coating on chloride threshold (Cl_{th}) of FBE coated steel rebars, the lollipop specimens were prepared with FBE coated steel with damaged coating. For this, the coating on the top of the ribs at the central 50 mm (1.96 in.) length of five FBE coated steel rebars were scratched off on both faces to create the damage as shown in Figure 2(c). The exposure and measurements were done, as explained earlier. Upon initiation of corrosion,

mortar of about 0.5 mm (0.019 in.) depth adjacent to uncoated steel and coated steel was powdered and collected. The chloride concentration in the powdered mortar was determined using chemical tests as per the guidelines prescribed in SHRP-330 [67]. For specimens with uncoated steel rebars, the chloride concentration in the mortar adjacent to the steel was the chloride threshold. However, chloride concentration at the coating-mortar interface ($Cl_{C\text{-}M}$) does not participate in the corrosion activities of the underlying steel of FBE coated steel rebar. Therefore, chloride concentration at the steel-coating interface was determined by using the EDX technique [34,61]. The chloride concentration at Location 6 in the micrograph shown in Figure 6 is the Cl_{th} of FBE coated steel rebars. To avoid the detection of chlorides from unknown depths in the coating, the chloride concentration was determined at the cross-section of the coating surface (and not beneath the FBE coating). The chloride concentration determined using EDX is in % by weight of the substrate (i.e., FBE coating). To convert this to %bwob, the chloride concentration in coating at coating-mortar interface (say, Location 1 in Figure 6) was considered equal to the chloride concentration in the mortar at the coating-mortar interface (which is in terms of %bwob). Then, the relative chloride concentrations in %bwob were determined at the steel surface and was the chloride threshold of FBE coated steel rebars.

3.2.3 Proposed framework for estimation of service life of RC systems with FBE coated steel rebars

Figure 7(a) shows the schematic with two-stage diffusion of chloride through concrete and coating. A MATLAB® program based on diffusion of chlorides through concrete [68] was modified to accommodate the diffusion of chlorides through FBE coating. Figure 7(b) shows that at age, t_0 of RC systems, the chloride concentration at the concrete surface is zero. At this age, the chloride concentrations at the coating surface is also zero. Therefore, no diffusion of chlorides can take place. At age t_1, the accumulated chloride concentration at the concrete, coating, and steel surfaces are $C_{S,\,ti}$, $C_{C\text{-}M,\,ti}$, and $C_{S\text{-}C,\,ti}$. As a result of chloride concentration

gradient at concrete, coating, and steel surface, chlorides diffuse through the concrete and FBE coating. At this stage, the chloride concentration at steel surface is less than the Cl_{th} of FBE coated steel rebars. Therefore, corrosion does not initiate. Later, at age t_{SL}, the accumulated chloride concentration at the steel surface is equal to the Cl_{th} of FBE coated steel rebars, results in the initiation of corrosion. In the present study, the time required for the chlorides to reach the steel surface through concrete and coating to the concentration equal to the Cl_{th} is defined as the service life of RC systems with FBE coated steel rebars. To estimate the service life of such RC systems, the input parameters determined from this study [FBE coating thickness ($t_{coating}$), $D_{cl,\ coating}$, and Cl_{th} of coated steel rebars] and other concrete properties [maximum surface chloride concentrations of concrete, D_{cl} of concrete, maturity constant (m) of concrete, concrete cover thickness (x)] presented elsewhere [63] were used.

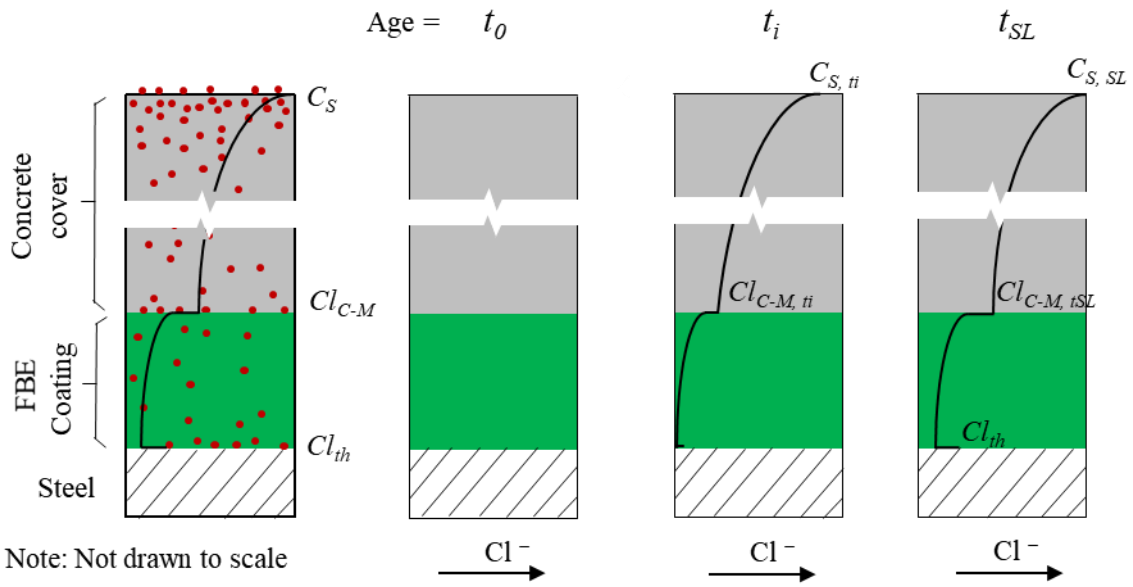

(a) Instantaneous chloride concentrations at various location in a FBE coating

(b) Framework to determine service life of RC systems with coated steel rebars

Figure 7 Proposed framework to determine the service life of RC system with FBE coated steel rebars

4 RESULTS AND DISCUSSION

This section provides the experimental results on showing the feasibility of HCP, MC current, LPR, and EIS to detect the initiation of corrosion in FBE coated steel rebars embedded

in cementitious systems. Then, by using the proposed test methodology, the initiation of corrosion in FBE coated steel rebar is detected. Also, the diffusion coefficient of FBE coating ($D_{cl,\ coating}$) and chloride threshold (Cl_{th}) of FBE coated steel rebars embedded in cementitious systems is determined by using the proposed framework. Then, these parameters and proposed framework is used to estimate the service lives of RC systems with FBE coated steel rebars.

4.1 Phase 1: Evaluation of various corrosion testing techniques

4.1.1 Half-cell potential (HCP)

Figure 8(a) shows the variation of HCP for uncoated steel rebars embedded in macrocell specimens. The horizontal dash line indicates the limit indicating more than 90% probability of corrosion for uncoated steel rebars as per ASTM G876. For each specimen, when the HCP drops below $-270\ mV_{SCE}$, the exposure to chloride solution was stopped, and macrocell specimens were autopsied. The initiation of corrosion was confirmed by visual observation of corroded steel surfaces. Whereas, Figure 8(b) shows the variation of HCP measured for one year obtained from specimens with FBE coated steel rebars with no damage (FBEC-ND). The HCP values were found to be varying from -100 to $-700\ mV_{SCE}$, throughout the exposure time. The vertical dash line represents that the initiation of corrosion was detected on or before 150 days of exposure time by EIS technique, which is discussed later. Therefore, the existing criteria for detecting initiation of corrosion using HCP, which is meant for uncoated steel rebars, may not be valid for detecting the initiation of corrosion in RC system with FBE coated steel rebars. The resistance of FBE coating is, $R_{coating}$ is significantly high. Therefore, the ohmic drop across the coating during HCP measurements will be high, making it difficult to capture the true response from steel surface underneath the FBE coating.

Figure 8(c) shows that the HCP measurements for macrocell specimens with FBEC-SD steels were found to be more positive than $-270\ mV_{SCE}$ for about 100 days of exposure to

chloride solution. The HCP value for FBEC-SD3 and SD5 dropped below – 270 mV_{SCE} – indicating the initiation of corrosion, which was confirmed with autopsied macrocell specimen. At the same time, FBEC-SD1 and SD5 were also autopsied, and it was found that the corrosion was initiated at the scratch damage locations in all the rebars. However, it was not evident from HCP measurements. To validate the unsuitability of ASTM C876 to detect the initiation of corrosion in FBE coated steel rebars, Specimen FBEC-SD2 was exposed to chloride solution, and HCP measurements were monitored. It was found that the HCP measurements were not always more negative than – 270 mV_{SCE}. It can be concluded that the interpretation of HCP measurements using ASTM C876, which is meant to be for RC systems with uncoated steel rebars, do not represent the corrosion activity of RC systems with FBE coated steel rebars.

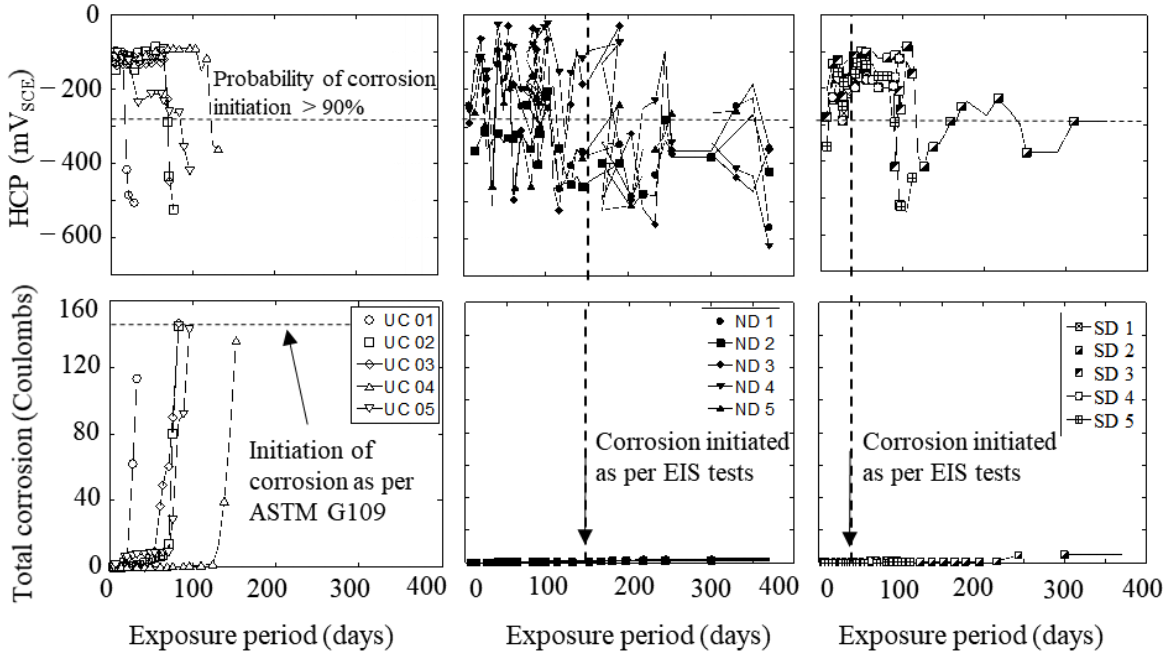

(a) Uncoated steel **(b) FBE coated steel (possibly with holidays)** **(c) Damaged FBE coated steel**

Figure 8 Calculated total corrosion and measured half-cell potentials from macrocell specimens

Figure 9 shows the corroded steel surface of FBEC-SD4 specimens. Here, HCP values of two out of four specimens were not in agreement with corrosion activities at FBEC-SD steel

rebars. The corrosion activities of two specimens might have got detected due to the placement of SCE on the mortar surface right above the location of the damage in the coating. Similarly, Pincheira et al. (2015) reported that the corrosion activities of RC systems with FBE coated steel could be detected only at the locations with high ionic conductivity between steel surface and the reference electrode (damage, delamination with cracks, etc.) [69]. In reality, the locations of damage are not known. Also, in later stage, the steel at the damage location can become the cathode and anodic reaction can continue under the coating [70,71]. Considering the high resistivity of the FBE coating, the measurements made on top of the concrete surface will not capture the corrosion activities beneath the coating. Therefore, the present study highly recommends not to rely on the existing criteria-based HCP measurements for detecting the initiation of corrosion in FBE coated steel rebars embedded in concrete.

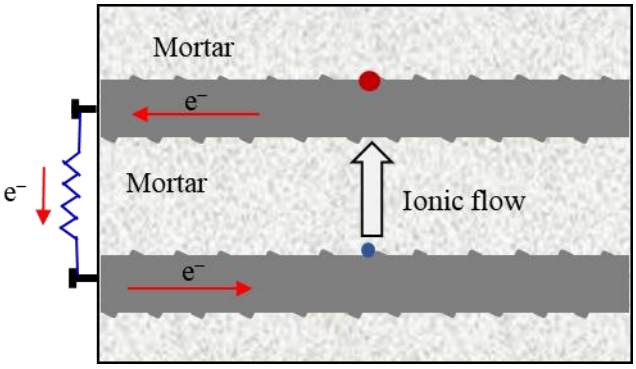

(a) Macrocell corrosion across uncoated steel rebars

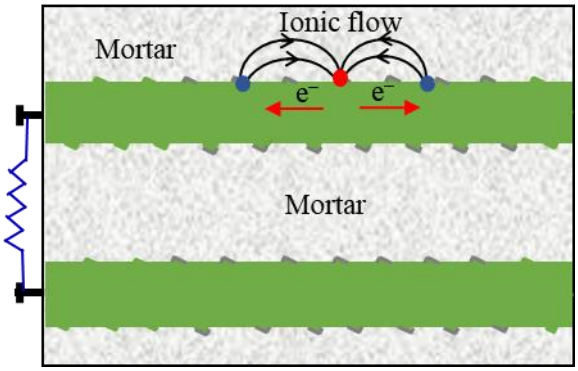

(b) Macrocell in same rebar with damage or pinholes

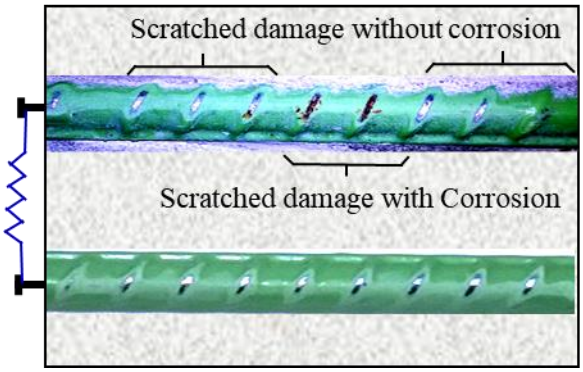

(c) Corrosion mechanism in FBE coated steel rebars with damage

Figure 9 Difference in the macrocell corrosion circuits (see arrows) in cases of uncoated and damaged FBE coated steels embedded in mortar/concrete

4.1.2 Macrocell corrosion (MC) current

Figure 8(a) shows the total corrosion calculated for macrocell specimens with uncoated steel rebars. The horizontal dash line represents the limit of 150 C prescribed by ASTM G109, indicating the initiation of corrosion. The calculated total corrosion values spiked to 150 C at the same instance when HCPs dropped below – 270 mV_{SCE}. This indicates the good agreement

between initiation of corrosion and criteria prescribed in ASTM G109 and ASTM C876 for the specimens with uncoated steel rebars. The initiation of corrosion was confirmed with autopsied macrocell specimens. Figure 8(b) and (c) show the total corrosion for macrocell specimens with FBEC- ND and FBEC-SD steels, respectively. Here, very low corrosion or no detectable pattern in the total corrosion was observed even after one year of exposure to 15% NaCl solution. However, the onset of corrosion was detected using EIS based test method after about 100 days of exposure to chloride solution, which is discussed later. However, the exposure of macrocell specimens to chloride solution and testing was continued for more than one year to confirm that the existing criteria on HCP and MC current measurements do not show detectable patterns even after prolonged exposure to chloride solution and corrosion.

Figure 9(a) and (b) show the difference in the macrocell corrosion circuits in the case of uncoated and FBE coated steel rebars. The resistance offered by FBE coating is significantly high; hence, the corrosion cell forms across various points in the top rebar itself – without the participation of another (bottom) rebars. Such corrosion may not be reflected in the MC current measurements made across the resistor (see Figure 9 (a) and (b)) in the ASTM G109 type MC current tests. Likewise, because of the high ohmic drop across the FBE coating, the HCP measurements made using ASTM C876 did not reflect the true corrosion activities at the steel surface. Similar concerns were also raised by researchers to highlight the challenges associated with existing criteria on the interpretation of HCP measurements of uncoated [28] and coated steel rebars [30,72] embedded in concrete. Figure 9(c) shows visible corrosion of steel on the scratches at the center of the rebar and possible formation of localized corrosion cell – proving the inadequacy of MC current measurements in detecting the ongoing corrosion in coated rebars. This also shows that only one rebar is required for the assessment of FBE coated steel rebars. Therefore, lollipop specimens were cast to evaluate the suitability of LPR and EIS [see Figure 4].

4.1.3 Linear polarization resistance (LPR)

Figure 10 shows the variation of $1/R_p$ obtained from lollipop specimens with FBEC-ND steels, which include LPR and EIS data. Measurements using LPR (circular markers) failed to detect the initiation of corrosion (no rise in $1/R_P$). Measurements using EIS (square markers) indicated a rise in $1/R_P$ of steel-coating interface at the time of initiation of corrosion. Further details on the efficiency of the EIS technique will be discussed in the next subsection with another set of test specimens. Also, photographs of FBEC-ND steel rebars from lollipop specimens in Figure 10 show that the time of autopsy of specimens was not the time of initiation of corrosion – indicating that the LPR measurements could not detect the initiation of corrosion. A small peak in $1/R_P$ was observed in case of FBEC-ND4 where the FBE coating was found to be cracked due to expansive force exerted by corrosion products. The cracked locations in the coating could have provided a path for ionic conduction and electrochemical measurements. In large scale RC systems, the location of corrosion, disbondment, and cracking of coatings are not known. Also, the high resistance of FBE coating in remaining locations, makes it impossible for LPR to get a response from underlying steel rebars, irrespective of ongoing corrosion. Similar conclusions were made by [37,73] for steel embedded in highly resistive concrete systems. Note that the resistance to polarization (R_P) using the LPR technique is the combined response from mortar, coating, and steel-coating interface [37,40]. Therefore, the effect of reduction in resistance to the polarization of the steel-coating interface could be significantly less to be detected in the change of total R_P.

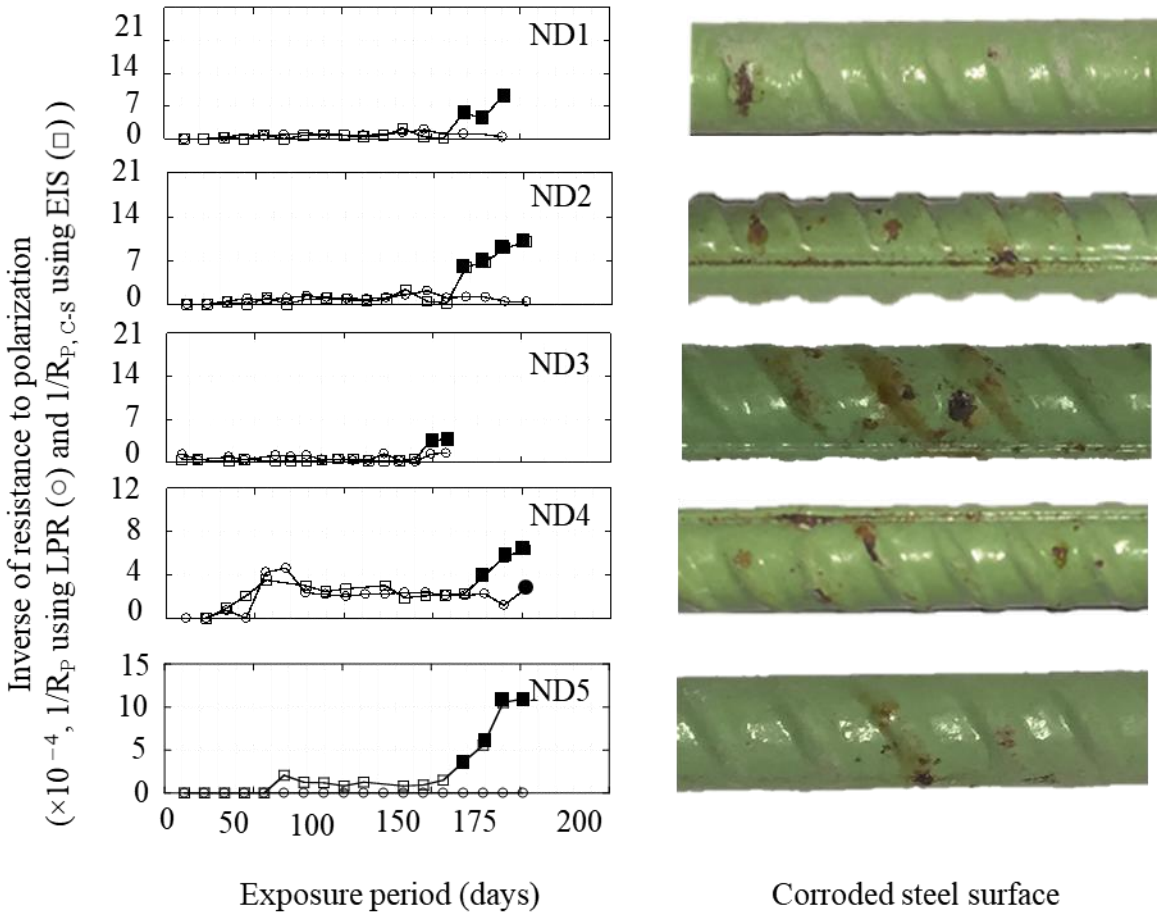

Figure 10 LPR and EIS measurements, and photographs of corroded FBE coated steel rebar surfaces after three cycles of detection of initiation of corrosion using EIS tests

4.1.4 Proposed methodology based on Electrochemical impedance spectroscopy (EIS)

Figure 11 shows the ideal Nyquist plot from FBEC-ND steel rebar embedded in cementitious systems and the ECC. Testing based on the EIS technique can capture responses from each element of the working electrode/test specimen (i.e., mortar, coating, and steel-coating interface). As shown, the response has three pure loops, corresponding to mortar, FBE coating, and steel-coating interface (S-C). The EEC was modified from [23,64,74,75] and used in this study. The response were analyzed, and resistance offered by each layer (mortar, coating, and steel-coating interface) were quantified using the EEC. In Figure 11, R_S is the resistance of the electrolyte solution; CPE_M and R_M are the capacitance and resistance of the mortar, respectively; CPE_C and R_C are the capacitance and resistance of the coating, respectively. In the present study, R_C was monitored throughout the testing to assess the

degradation of FBE coating due to moisture and chloride ingress. The CPE_{S-C} and $R_{P,\,S-C}$ are the capacitance and resistance of polarization of the steel-coating (S-C) interface, respectively. To verify the reliability and stability of EIS results, the error in the fitting of each component was restricted to 20%, and the overall chi-square value was maintained below 0.005 by using Kramers-Kronig Transformations (KKT) [43]. This enables the monitoring of resistance of coating (R_C), resistance to the polarization of steel-coating ($R_{P,\,S-C}$), and detecting initiation of corrosion. Therefore, monitoring the response from the steel-coating interface ($R_{P,\,S-C}$) could detect the initiation of corrosion. Note that R_M was not monitored in this study because the same mortar was used for all the specimens.

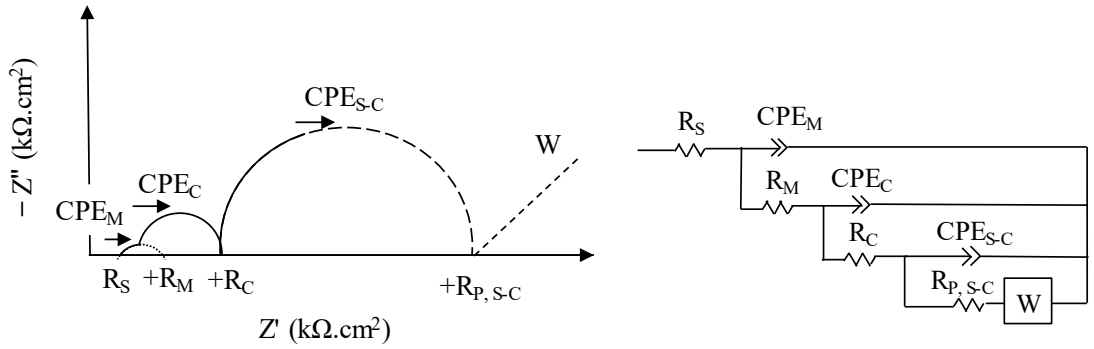

(a) Ideal Nyquist plot **(b) Equivalent electrical circuit (EEC)**

Figure 11 Ideal EIS response from FBE coated steel rebar embedded in the cementitious system and corresponding EEC

4.1.4.1 Degradation of FBE coating

Figure 12 demonstrates four stages of coating degradation and corresponding Nyquist plots obtained from lollipop specimens with FBE coated steel embedded in mortar and exposed to chloride solution. Figure 12 (a) shows the Nyquist plot obtained from lollipop specimen with FBE coated steel rebar with an initial exposure period (Stage 1). It consists of three loops. First, second, and third loops corresponding to cementitious mortar [not visible in Figure 12 (a)], FBE coating, and steel-coating interface, respectively. At this stage, the impedance modulus of the steel-coating interface at low-frequency was found to be significantly high (10^3

– 10^4 kΩ.cm^2). Therefore, the response from the steel-coating interface is a pure loop with high resistance – indicating that the FBE coating has a barrier layer and prevents the ingress of moisture/oxygen/chlorides [48]. The schematic of steel-coating-concrete in Figure 12(a) describes that the FBE coating is not degraded, and resists the ingress of pore solution – resulting in no corrosion activities at the steel surface.

Figure 12 (b) shows that with further exposure, the resistance of FBE coating and steel-coating interface decreases (Stage 2). During this stage, the FBE coating may have degraded due to ingress of moisture and chlorides [see schematic in Figure 12 (b)]. Therefore, the resistance of the FBE coating was decreased from ≈ 40 kΩ.cm^2 to ≈ 20 kΩ.cm^2. At this stage, the low-frequency impedance modulus of the steel-coating interface was high (10^2–10^3 kΩ.cm^2) – indicating that the steel surface may remain electrochemically inactive due to unavailability of sufficient oxygen and moisture at the steel surfaces.

Figure 12 (c) shows that the resistance offered by FBE coating was increased from 20 kΩ.cm^2 to 30 kΩ.cm^2 (Stage 3). This increase in R_C can be attributed to the filling of pores in coating at the steel-coating interface with insoluble corrosion products (Fe_XO_Y). These insoluble corrosion products increase the resistance of coating due to their insulating nature [48,76]. Due to the formation of insoluble corrosion products at the steel-coating interface, the moisture may not reach the steel surface. As a result, the $R_{P,\,S\text{-}C}$ of the steel-coating interface was found to increase by about 70% of $R_{P,\,S\text{-}C}$ during Stage 2. Figure 13(a) shows the evidence on the filling of corrosion products in the pores at the steel-coating interface. The EDX response from the corrosion products did not have chlorides in it – indicating the formation of Fe_XO_Y corrosion products, which are insoluble in nature.

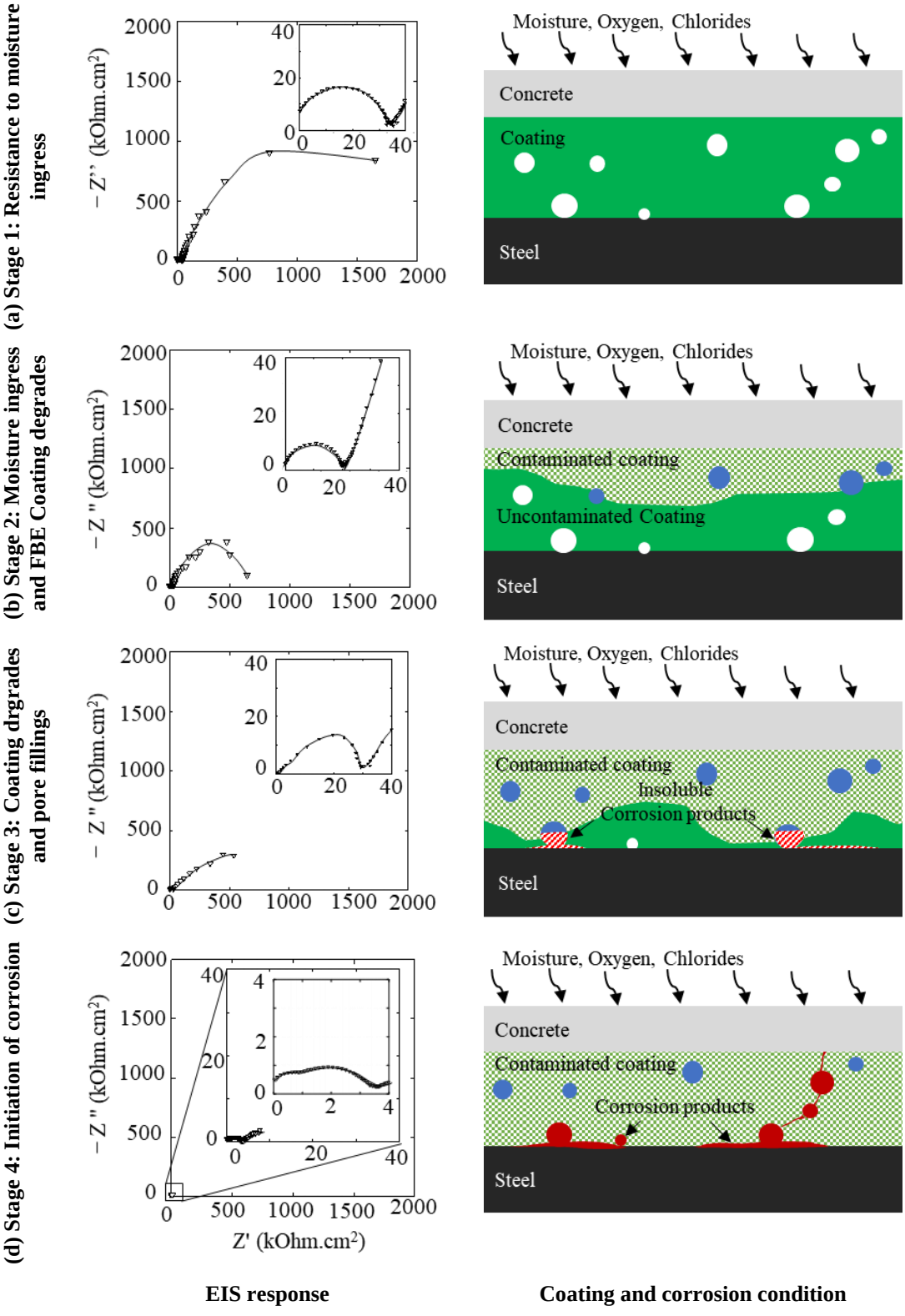

Figure 12 EIS response from lollipop specimens with FBE coated steel at various stages during exposure to chloride solution

With further exposure when moisture with chlorides reaches the steel surface, the entrapped corrosion products may move out of pores due to radially outward pressure by the

new corrosion products with chloride (Fe_XCl_Y), which are soluble in water. These corrosion products may fill the available pore space in coating and move out of the thin coating film. These corrosion products can get absorb moisture and provide a low resistance path – resulting in the gradual reduction of resistance of the coating and a significant reduction in resistance to the $R_{P,\ S\text{-}C}$ (i.e., Stage 4). Figure 12 (d) shows the Nyquist plot, where R_C and $R_{P,\ C\text{-}S}$ is significantly low as compared to that obtained in Stage 1, 2, and 3. The schematic in Figure 12 (d) shows the significant degradation of coating and initiation of corrosion due to chlorides at the steel surface. The initiation of corrosion and corrosion products were confirmed by the micrograph and EDX analysis of corrosion products [see Figure 13 (b)].

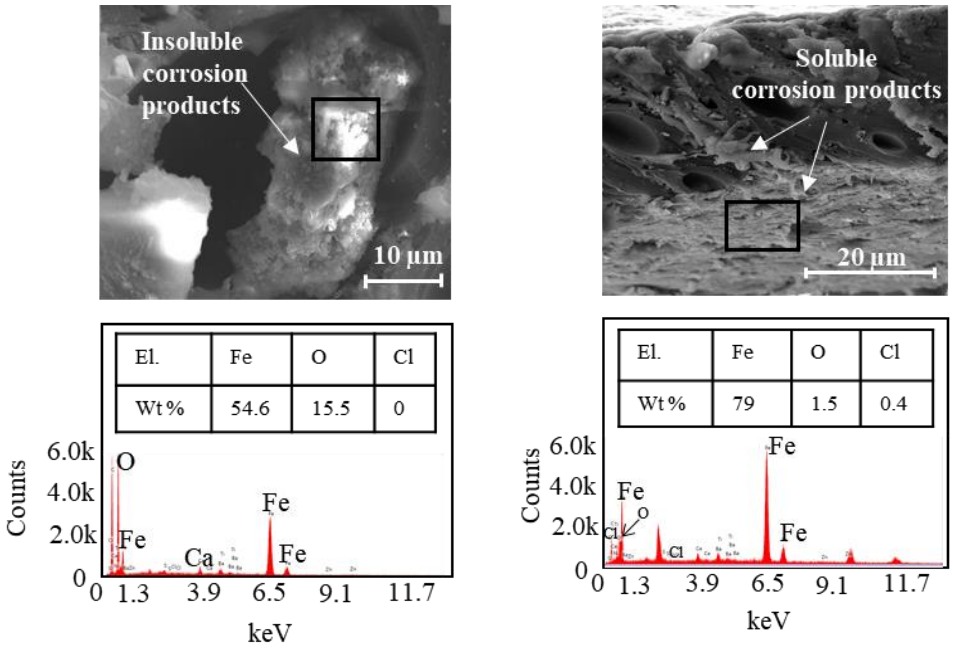

(a) Insoluble corrosion products (without chlorides) filled in coating – Stage 3

(b) Soluble corrosion products (with chlorides) oozing out of coating – Stage 4

Figure 13 Evidence of corrosion products filled in pores of FBE coating [Note: other elements such as C, Ba, Ca, Ti, and Zn are not shown in the EDAX analysis]

Figure 14(a) shows the relative coating resistance of FBE coating at various exposure time. The relative coating resistance was obtained by normalizing the resistance of coating at time 't' to the R_C at the starting of the exposure. The R_C was found to follow a trend in four

stage. The same is summarized in the schematic with changes in coating pore structures and typical coating resistance trend shown in Figure 14(b). The relative resistance of coating after about 160 days of exposure was reduced to ≈ 0. The resistance of coating has got reduced significantly due to the specimens were exposed to one additional cyclic exposure after the initiation of corrosion was detected. The specimens were exposed to one additional cycle to confirm the initiation of corrosion. This might have lead to the propagation of corrosion – resulting in microcracks in the coating due to radially outward forces generated by additional corrosion products with a larger volume than the volume of steel. These microcracks may lead to the shortcircuit between the underlying steel and measurement tool. Therefore, the overall resistance of coating may not be zero, but due to localized cracking and shortcircuiting, the R_C may show as zero.

The FBE coating degradation is proposed to be a 4-stage degradation when exposed to an alkaline solution with chlorides. Stage 1 is defined when R_C was constant for a few weeks of exposure – indicating that the FBE coating could resist the ingress of moisture for about three to four weeks. The unfilled elliptical empty pores in the schematic represent that the pore solution could not penetrate through the coating. Stage 2 is defined when R_C started to decrease due to ingress of pore solution (possibly with chlorides) in FBE coating to some depth of the coating – resulting in the decrease in the R_C of FBE coating. On availability of moisture and oxygen, insoluble corrosion products may form and fill the pores at the steel-coating interface – increasing R_C, defined as Stage 3 [34] [see Figure 13 (a)]. Subsequently, with further exposure when pore solution and chlorides reach the steel surface, corrosion may progress due to the availability of chlorides, moisture, and oxygen. These corrosion products may exert radial pressure on coating and may result in cracking. Therefore, Stage 4 is defined when R_C continues to decrease due to the increase in the interconnectivity of pores and cracks.

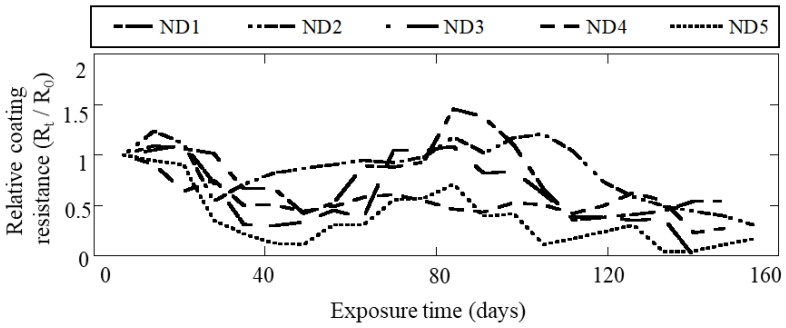

(a) Relative coating resistance

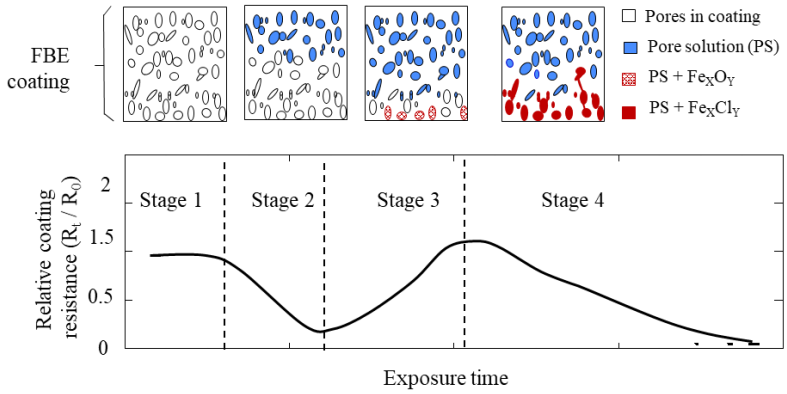

(b) Changes in coating pore structure and mechanism of degradation of coating

Figure 14 Proposed 4-stage coating degradation process

4.1.4.2 Initiation of corrosion

Figure 15 shows the variation of $1/R_{P,\,S\text{-}C}$ for FBEC-ND and FBEC-SD specimens. The $1/R_{P,\,S\text{-}C}$ for values for FBEC-ND, showed a spike up for all the specimens at around 40 days of exposure. This can be attributed to the formation of oxide/passive layer (Fe_XO_Y) on the steel surface. However, once these insoluble corrosion products are formed, steel rebars remain passive until the chlorides reach to the rebar surface. The larger visible spikes in the $1/R_{P,\,C\text{-}S}$ at about 150 days of exposure for FBEC-ND and at about 50 days for FBEC-SD specimens represent the initiation of corrosion, illustrated with the filled markers. Note that the rate of corrosion of FBEC-SD specimens were about one order higher than that of FBEC-ND steel rebars.

Upon initiation of corrosion was detected using statistical analysis of $1/R_{P,\,S\text{-}C}$, the specimens were autopsied and visually inspected. For FBEC-ND steels, corrosion was not

visible on the coating surface of FBE coated steels extracted from lollipop specimens [see Figure 16(a)]. The coated steels were cut at various locations, for example, Section 1-1 to 5-5. The initiation of corrosion was confirmed by visible underfilm corrosion in the coated steels. Figure 16(a) shows the enlarged image of the cross-sections with corrosion under the coating. Similarly, Figure 16(b) shows that the FBEC-SD coated steel rebar undergo pitting corrosion. It can be concluded that the proposed EIS based methodology can detect the initiation of corrosion in FBE coated steel rebars embedded in the cementitious system at the early stage. It is also observed that the FBE coated steel rebars with damaged coating can undergo premature initiation of corrosion with a significantly high rate of corrosion.

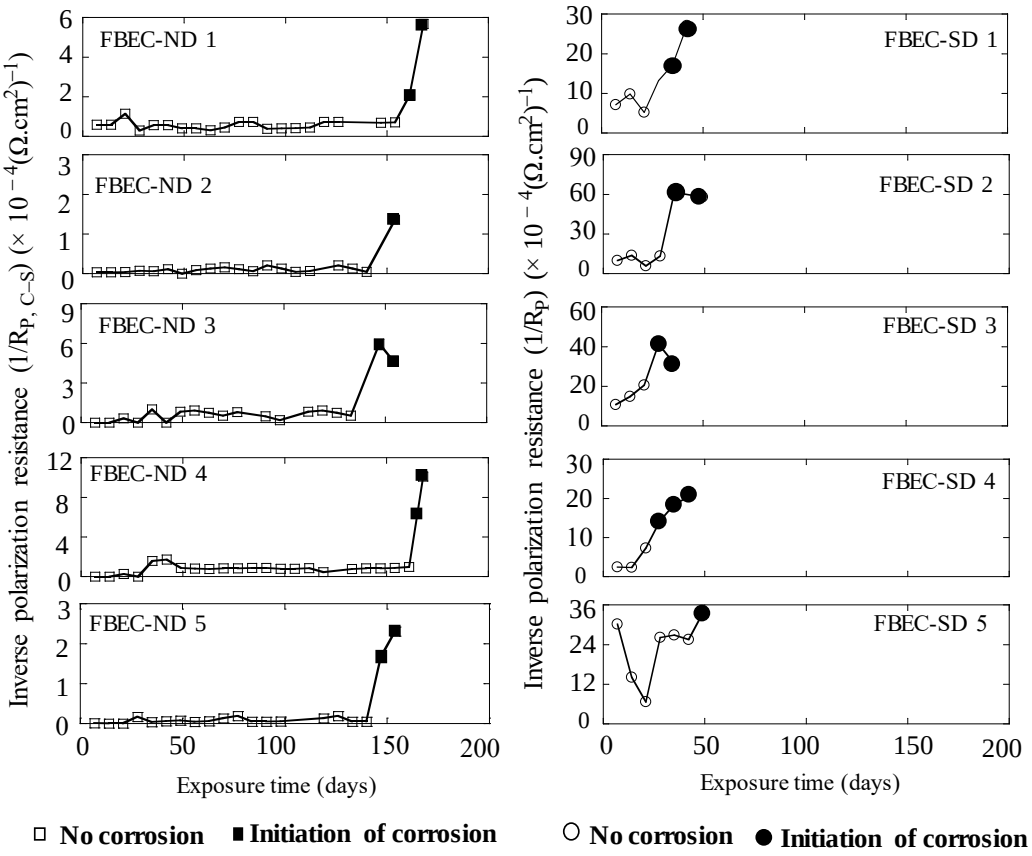

Figure 15 Detection of initiation of corrosion (unfilled and filled markers indicate passive and active corrosion measurements, respectively)

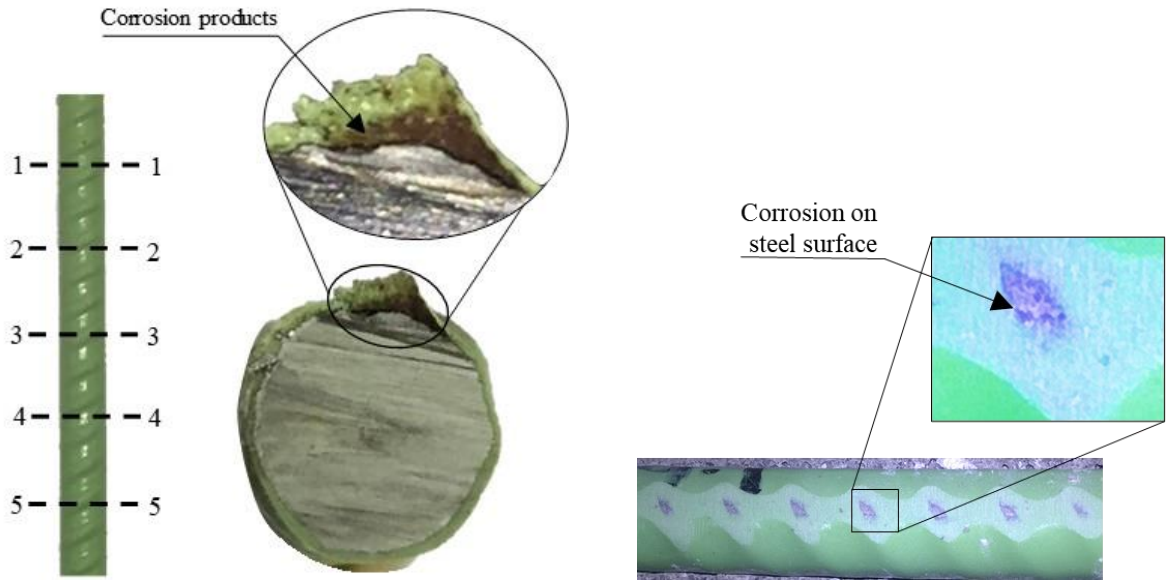

(a) Underfilm corrosion in FBE coated steel rebar with no damage to coating

(b) Localised corrosion pits on steel surface at locations with scratched location

Figure 16 FBE coated steel rebar extracted from a lollipop specimen after initiation of corrosion has been detected using EIS tests

4.2 Parameters to estimate the service life of RC systems with FBE coated steel rebars

4.2.1 Diffusion coefficients of coatings

The chloride profiles were obtained from five of the FBE coating samples and are presented elsewhere [58]. Among all the coating samples tested, the chloride concentration next to the exposed surface of coating was found to be significantly lower than the chloride concentration at the exposed surface of the coating. The significant ddifference in the chloride concentration can be attributed to the dense microstructure of FBE coating due to adequate curing during the coating process [77]. This closed microstructure can restrict the penetration of chloride in the coating. The average diffusion coefficient of FBE coating ($D_{cl,\ coating}$) was found to be $\approx$ LN (1.6, 0.25) $\times$ 10^{-20} m^2/s. The $D_{cl,\ coating}$ is significantly low, which can delay the transport of chloride in the coating.

4.2.2 Chloride thresholds

Figure 17 shows that the Cl_{th} of uncoated, FBEC-ND, and FBEC-SD steel specimens are 0.40, 0.12, and 0.22% bwob, respectively. The average Cl_{th} for uncoated steel rebars from macrocell specimens was found to be 0.39% bwob, which is comparable to the Cl_{th} obtained from lollipop specimens. Here, the Cl_{th} for FBE coated steel with no damage and FBE coated steel with scratch damage was found to be 70% and 50% less than the Cl_{th} of uncoated steel rebars, respectively. Note that the Cl_{th} of FBEC-ND is less than FBEC- SD because the Cl_{th} for FBEC-ND was determined from the chloride concentration in the coating interface at the steel-coating interface. On the other hand, for FBEC-SD, Cl_{th} was the chloride concentration in the mortar, which was in contact with the damaged locations. The initiation of corrosion in FBEC-SD specimens is not governed by the diffusion of chlorides through the coating. Therefore, the service life of RC system with FBEC-ND steel can be higher than FBEC-SD and uncoated steel rebars because the chlorides have to travel through the coating film with significantly low diffusion coefficients.

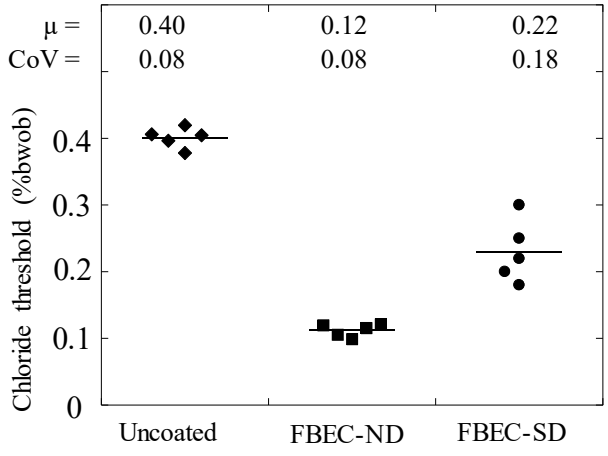

Figure 17 Chloride thresholds of uncoated, and FBE coated steel rebars with and without damage to coating

4.2.3 Coating thickness

Figure 18 shows that the coating thickness ($t_{coating}$) of FBE coated steel rebars varies from 100 μm to 1000 μm. The horizontal dash line at 175 μm and 350 μm are the lower and

the upper limit of $t_{coating}$ as specified by ASTM A775. The circular markers are the measured $t_{coating}$ of the FBE coated steel rebars at locations between two ribs and on the top of ribs. It was found that the $t_{coating}$ at most of the locations exceeded the permissible limits specified by ASTM A775. The $t_{coating} > 350$ µm can result in a significant reduction in bond strength [78,79] and the $t_{coating} < 175$ µm can lead to premature initiation of corrosion [78]. However, some of the standards or guidelines recommend minimum $t_{coating}$ as 100 µm [80]. Therefore, a parametric study was conducted, and the effect of coating thickness on time to initiation of corrosion was estimated, which is discussed next.

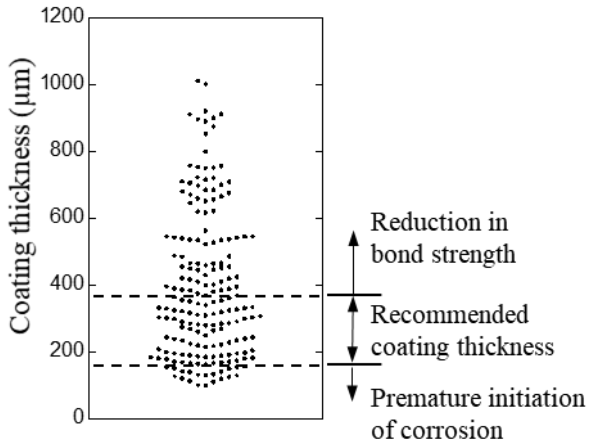

Figure 18 Variation of coating thickness in FBE coated steel rebars

4.3 Estimation of service life

Figure 19 shows the cumulative distribution function for the time to initiation of corrosion in RC systems with uncoated, FBEC-SD, and FBEC-ND steel rebars with a $t_{coating}$ of 300 µm, 200 µm, and 100 µm. It was found that the service life for RC systems with FBEC-ND steel rebars with $t_{coating}$ of 200 and 100 µm was about 30 and 50% less than the service life of RC systems with FBE coated steel rebars with $t_{coating}$ of 300 µm, respectively. The service life of RC system with FBE coated steel rebars with $t_{coating}$ of 100 µm was only about 20% more than that of t_i for RC systems with uncoated steel rebars. Note that the coating of the coated steel rebars gets damaged due to poor construction practices. Therefore, the service life for RC

systems with FBEC-SD rebars was estimated and it was found to be 35% less than the service life of RC systems with uncoated steel rebars.

$D_{cl,\ concrete}$ ($\times 10^{-11}$ m^2/s)	=	LN (7.1, 0.3)
C_{max} (% bwob)	=	LN (1.16, 0.03)
x (mm)	=	LN (50, 10)
m	=	0.38
$D_{cl,\ coating}$ ($\times 10^{-20}$ m^2/s)	=	LN (3.6, 0.70)

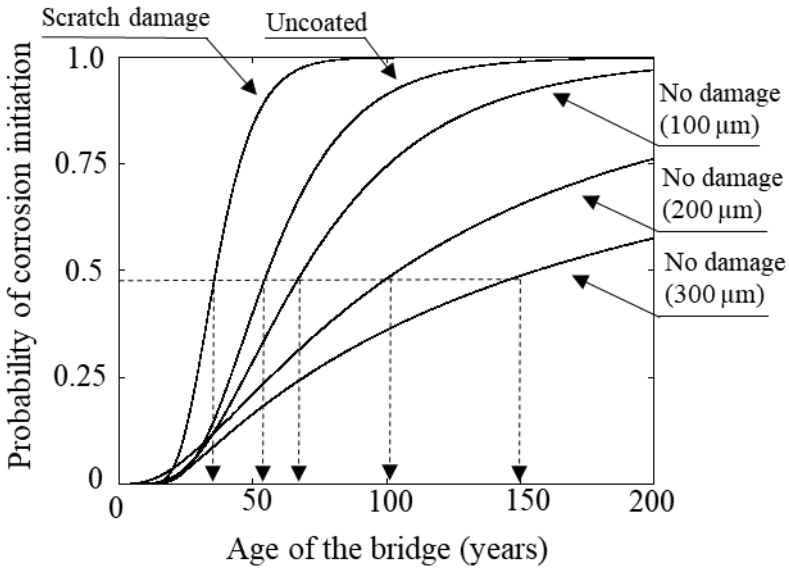

Figure 19 Effect of coating thickness and damage to coating on the service life of RC structures with FBE coated steel rebars

5 RECOMMENDATIONS

Based on the experimental results, the following recommendations are made for FBE coated steel rebars:

- Test method based on EIS should be used to detect the initiation of corrosion in RC systems with FBE coated steel rebars
- No single recorded coating thickness measurement shall be less than 0.8 times the specified minimum thickness or more than 1.2 times the specified maximum thickness.
- The allowable damage level in coating = zero; no damage to coating should be acceptable
- The R_C of FBE coating > 1×10^3 kΩ.cm^2

6 CONCLUSIONS

Detection of corrosion initiation in reinforced concrete (RC) systems with fusion-bonded-epoxy (FBE) coated steel rebars is challenging due to the unavailability of the suitable test method. For this, test methods with existing techniques such as half-cell potential, macrocell corrosion current, linear polarization resistance, and electrochemical impedance spectroscopy (EIS) were assessed. Experimental investigations show that only test method based on EIS could detect the initiation of corrosion. Repeated measurement of resistance of coating (R_C) reveals that the degradation of FBE coating is a four-stage process. Based on cyclic wet-dry exposure of lollipop specimens, repeated EIS (Nyquist and Bode plots) measurements, statistical analysis of $1/R_{P,\ S\text{-}C}$, and chemical & EDX tests, the chloride thresholds (Cl_{th}) for uncoated, FBEC-ND, and FBEC-SD steel rebars were determined to be 0.40, 0.12, and 0.22 %bwob, respectively. The Cl_{th} of uncoated steel rebar was double of the Cl_{th} of FBEC-SD steel rebars. Also, it was about four times the Cl_{th} of FBEC-ND steel rebars. Also, a framework was proposed to estimate the service life of RC structures with FBE coated steel rebars by considering the diffusion of chlorides through concrete and coating, and the Cl_{th} of coated steel rebars at coating-steel interface. Based on the results from this paper ($D_{cl,\ coating,}$ and Cl_{th}), and other concrete properties, a case study was conducted, the service life of RC systems. The service life of RC system with FBE coated steel with a coating thickness of 200 and 100 µm was about 30% and 50% less than the service life of RC systems with FBE coated steel with coating thickness of 300 µm. Whereas, the service life RC systems with FBE coated steel rebars with damage was found to be 35% less than the service life of RC systems with uncoated steel rebars, which is about 70% less than RC systems with FBE coated steel rebars. The present study recommends avoiding the usage of FBE coated steel rebars unless adequate coating thickness can not be achieved and damage to coating can not be avoided.

7 ACKNOWLEDGMENTS

The authors acknowledge the financial support (Project No. EMR/2016/003196) received from the Science and Engineering Research Board, Department of Science and Technology and the partial financial support from the Ministry of Human Resource Development of the Government of India. The authors also acknowledge assistance from the faculty, laboratory staff, and students in the Construction Materials Research Laboratory in the Department of Civil Engineering, Indian Institute of Technology Madras, Chennai, India.

8 REFERENCES

[1] T. Monetta, F. Bellucci, L. Nicodemo, L. Nicolais, Protective properties of epoxy-based organic coatings on mild steel, Prog. Org. Coatings. 21 (1993) 353–369. https://doi.org/10.1016/0033-0655(93)80050-K.

[2] D. McDonald, Epoxy-Coated Reinforcing Steel Bars in Northern America, Epoxy Interes. Gr. CRSI. (2009).

[3] A. Griffith, H.M. Laylor, Epoxy Coated Reinforcement Study, Oregon, 1999.

[4] W.A. Pyć, R.E. Weyers, M. Weyers, D.W. Mokarem, J. Zemajtis, Field performance of epoxy-coated reinforcing steel in virginia bridge decks, Virginia Department of Transportation, Charlottesville, Virginia, 2000.

[5] J. Zemajtis, R.E. Weyers, M.M. Sprinkel, An Evaluation of the Performance of Epoxy-Coated Reinforcing Steel in Concrete Exposure Specimens, Final Contract Rep. by Virginia Transp. Res. Counc. (1998) 147 p.

[6] G.R. Kim, S.H. Lee, H.Y. Song, J.M. Han, Electrochemical characterization of epoxy coated steel under cathodic protection, in: NACE Corros. Conf. Expo, 2007: pp. 1–13.

[7] F. Fanous, H. Wu, Performance of Coated Reinforcing Bars in Cracked Bridge Decks, J. Bridg. Eng. 10 (2005) pp 255-261. https://doi.org/10.1061/(ASCE)1084-

0702(2005)10:3(255).

[8] F. Pianca, H. Schell, G. Cautillo, The performance of epoxy coated reinforcement : experience of the Ontario ministry of transportation, Int. J. Mater. Prod. Technol. 23 (2005) 286–308.

[9] A.A. Sagüés, K. Lau, R.G. Powers, R.J. Kessler, Corrosion of epoxy-coated rebar in marine bridges - A 30 year perspective, CORROSION. 66 (2010) 065001-.

[10] A.A. Sagues, R.G. Powers, Effect of Concrete Environment on the Corrosion Performance of Epoxy-Coated Reinforcing Steel, Corrosion/90. Paper No. (1990).

[11] K.Z. Kahhaleh, E. Vaca-cortés, J.O. Jirsa, H.G. Wheat, R.L. Carrasquillo, Corrosion performance of epoxy-coated reinforcement – macrocell tests, Texas, USA, 1998.

[12] R.N. Swamy, S. Koyama, Epoxy Coated Rebars The Panacea for Steel Corrosion in Concrete, Constr. Build. Mater. 3 (1989) 86–91.

[13] M.S.H.S. Mohammed, R.S. Raghavan, G.M.S. Knight, V. Murugesan, Macrocell Corrosion Studies of Coated Rebars, Arab. J. Sci. Eng. 39 (2014) 3535–3543. https://doi.org/10.1007/s13369-014-1006-x.

[14] W.T. Scannell, K.C. Clear, Long-Term Outdoor Exposure Evaluation of Concrete Slabs Containing Epoxy-Coated Reinforcing Steel, Transp. Res. Rec. (1990) 70–78.

[15] R. Vedalakshmi, K. Kumar, V. Raju, N.S. Rengaswamy, Effect of prior damage on the performance of cement based coatings on rebar: Macrocell corrosion studies, Cem. Concr. Compos. 22 (2000) 417–421. https://doi.org/10.1016/S0958-9465(00)00041-X.

[16] A.A. Sohanghpurwala, K.C. CLEAR, Effectiveness of Epoxy Coatings in Minimizing Corrosion of Reinforcing Steel in Concrete, (1990) 193–204.

[17] D.G. Manning, Corrosion performance of epoxy-coated reinforcing steel: North American experience, Constr. Build. Mater. 10 (1996) 349–365. https://doi.org/10.1016/0950-0618(95)00028-3.

[18] C.M. Hansson, R. Haas, R. Green, R.C. Evers, O.K. Gepraegs, R. Al-Assar, Corrosion Protection Strategies for Ministry Bridges, 2000.

[19] S. Kessler, M. Zintel, C. Gehlen, Defects in epoxy-coated reinforcement and their impact on the service life of a concrete structure A study of critical chloride content and macro-cell corrosion, Struct. Concr. (2015) 398–405. https://doi.org/10.1002/suco.201400085.

[20] S. Kessler, U. Angst, M. Zintel, B. Elsener, C. Gehlen, Epoxy-coated reinforcement in concrete structures: Results of a Swiss pilot project after 24 years of field exposure, Mater. Corros. 67 (2016) 631–638. https://doi.org/10.1002/maco.201608863.

[21] E.V. Cortés, Corrosion Performance of Epoxy-Coated Reinforcement in Aggressive Environments, The University of Texas at Austin, 1998.

[22] O.S.B. Al-Amoudi, M. Maslehuddin, M. Ibrahim, Long-term performance of fusion-bonded epoxy-coated steel bars in chloride-contaminated concrete, ACI Mater. J. 101 (2004) 303–309.

[23] K. Lau, A.A. Sagüés, Coating Condition Evaluation of Epoxy-Coated Rebar, Electrochem. Soc. 3 (2007) 81–92.

[24] M.C. Brown, R.E. Weyers, M.M. Sprinkel, Service life extension of virginia bridge decks afforded by epoxy-coated reinforcement, J. ASTM Int. 3 (2006) 1–13. https://doi.org/10.1520/JAI11793.

[25] B. Goffin, Non-destructive detection of corrosion of epoxy coated rebars, Yhe University of British Columbia, Vancouver, 2017.

[26] ASTM C876, Astm C876: Standard Test Method for Half-Cell Potentials of Uncoated Reinforcing Steel in Concrete, 2015. https://doi.org/10.1520/C0876-09.2.

[27] S. Kessler, C. Gehlen, Reliability evaluation of half-cell potential measurement using POD, J. Infrastruct. Syst. 23 (2017). https://doi.org/10.1061/(ASCE)IS.1943-

555X.0000334.

[28] B. Elsener, C. Andrade, J. Gulikers, R. Polder, M. Raupach, Half-cell potential measurements - Potential mapping on reinforced concrete structures, Mater. Struct. Constr. 36 (2003) 461–471. https://doi.org/10.1617/13718.

[29] S. Kessler, C. Gehlen, Influence of Concrete Moisture Condition on Half-Cell Potential Measurement, Int. Conf. Durab. Concr. Struct. ICDCS 2016. 5th Intern (2016) 257–264. https://doi.org/10.5703/1288284316142.

[30] D.D.N. Singh, R. Ghosh, Unexpected Deterioration of Fusion-Bonded Epoxy-Coated Rebars Embedded in Chloride- Contaminated Concrete Environments, Corrosion. 61 (2005) 815–829.

[31] ASTM G109-07, Standard Test Method for Determining the Effects of Chemical Admixtures on the Corrosion of Embedded Steel Reinforcement in Concrete Exposed to Chloride Environments, West Conshohocken, USA, 2013. https://doi.org/10.1520/G0109-07R13.2.

[32] S. Rengaraju, A. Godara, P. Alapati, R.G. Pillai, Macrocell corrosion mechanisms of prestressing strands in various concretes, Mag. Concr. Res. 72 (2020) 194–206. https://doi.org/10.1680/jmacr.18.00284.

[33] C.M. Hansson, A. Poursaee, A. Laurent, Macrocell and microcell corrosion of steel in ordinary Portland cement and high performance concretes, Cem. Concr. Res. 36 (2006) 2098–2102. https://doi.org/10.1016/j.cemconres.2006.07.005.

[34] X.H. Wang, Y. Gao, Corrosion behavior of epoxy-coated reinforced bars in RC test specimens subjected to pre-exposure loading and wetting-drying cycles, Constr. Build. Mater. 119 (2016) 185–205. https://doi.org/10.1016/j.conbuildmat.2016.05.066.

[35] S.K. Lee, P.D. Krauss, Long-Term Performance of Epoxy-Coated Reinforcing Steel in Heavy Salt-Contaminated Concrete, FHWA-HRT-0 (2004).

[36] C. Andrade, Corrosion measurements in concrete structures and interpretation of data, Indian Concr. J. 94 (2020) 1–9.

[37] S. Rengaraju, L. Neelakantan, R.G. Pillai, Investigation on the polarization resistance of steel embedded in highly resistive cementitious systems e An attempt and challenges, Electrochim. Acta. 308 (2019) 131–141. https://doi.org/10.1016/j.electacta.2019.03.200.

[38] W.S. Tait, Corrosion Prevention and Control of Chemical Processing Equipment, in: Handb. Environ. Degrad. Mater. Second Ed., Second Edi, Elsevier Inc., 2012: pp. 863–886. https://doi.org/10.1016/B978-1-4377-3455-3.00028-6.

[39] A. Cao-Paz, A. Covelo, J. Farina, X.. R. Nóvoa, C. Pérez, L. Rodríguez-Pardo, Coatings Ingress of water into organic coatings : Real-time monitoring of the capacitance and increase in mass, Prog. Org. Coatings. 69 (2010) 150–157. https://doi.org/10.1016/j.porgcoat.2010.04.004.

[40] M.G. Fontana, Corrosion Engineering, 3rd editio, McGraw-Hill Book Company, Singapore, 1986.

[41] A. Miszczyk, K. Darowicki, Water uptake in protective organic coatings and its re fl ection in measured coating impedance, Prog. Org. Coatings. 124 (2018) 296–302. https://doi.org/10.1016/j.porgcoat.2018.03.002.

[42] N. Perini, A.R. Prado, C.M.S. Sad, E.V.R. Castro, M.B.J.G. Freitas, Electrochemical impedance spectroscopy for in situ petroleum analysis and water-in-oil emulsion characterization, Fuel. 91 (2012) 224–228. https://doi.org/10.1016/j.fuel.2011.06.057.

[43] X. Chen, W.L. Ebert, J.E. Indacochea, Electrochemical corrosion of a noble metal-bearing alloy-oxide composite, Corros. Sci. 124 (2017) 10–24. https://doi.org/10.1016/j.corsci.2017.04.010.

[44] A.A. Sagüés, A.M. Zayed, Low-Frequency Electrochemical Impedance for Measuring

Corrosion of Epoxy-Coated Reinforcing Steel in Concrete, Corrosion. 47 (1991) 852–859. https://doi.org/10.5006/1.3585197.

[45] F. Tang, Y. Bao, Y. Chen, Y. Tang, G. Chen, Impact and corrosion resistances of duplex epoxy/enamel coated plates, Constr. Build. Mater. 112 (2016) 7–18. https://doi.org/10.1016/j.conbuildmat.2016.02.170.

[46] F. Tang, G. Chen, J.S. Volz, R.K. Brow, M.L. Koenigstein, Cement-modified enamel coating for enhanced corrosion resistance of steel reinforcing bars, Cem. Concr. Compos. 35 (2013) 171–180. https://doi.org/10.1016/j.cemconcomp.2012.08.009.

[47] F. Tang, G. Chen, R.K. Brow, M.L. Koenigstein, Electrochemical Characteristics and Equivalent Circuit Representation of Mortar-Coating-Steel Systems by EIS, in: Corros. Conf., 2014: pp. 1–10.

[48] F. Tang, G. Chen, R.K. Brow, J.S. Volz, M.L. Koenigstein, Corrosion resistance and mechanism of steel rebar coated with three types of enamel, Corros. Sci. 59 (2012) 157–168. https://doi.org/10.1016/j.corsci.2012.02.024.

[49] A. Barbucci, M. Delucchi, L. Goretta, G. Cerisola, Electrochemical and physico-chemical characterization of fluorinated organic coatings for steel and concrete protection: Influence of the pigment volume concentration, Prog. Org. Coatings. 33 (1998) 139–148. https://doi.org/10.1016/S0300-9440(98)00049-6.

[50] A.A. Sagues, A.M. Zayed, Low-Frequency Electrochemical Impedance for Measuring Corrosion of Epoxy-Coated Reinforcing Steel in Concrete *, CORROSION. (1991) 852–859.

[51] M.G. Sohail, R. Kahraman, N.A. Alnuaimi, B. Gencturk, W. Alnahhal, M. Dawood, A. Belarbi, Electrochemical behavior of mild and corrosion resistant concrete reinforcing steels, Constr. Build. Mater. 232 (2020) 117205. https://doi.org/10.1016/j.conbuildmat.2019.117205.

[52] K. Tuutti, Service life of structures with regard to corrosion of embedded steel, (n.d.).

[53] R.G. Pillai, R. Gettu, M. Santhanam, S. Rengaraju, Y. Dhandapani, S. Rathnarajan, A.S. Basavaraj, Service life and life cycle assessment of reinforced concrete systems with limestone calcined clay cement (LC3), Cem. Concr. Res. 118 (2019) 111–119. https://doi.org/10.1016/j.cemconres.2018.11.019.

[54] R.G. Pillai, R. Gettu, M. Santhanam, Use of supplementary cementitious materials (SCMs) in reinforced concrete systems – Benefits and limitations, Rev. ALCONPAT. 10 (2020) 147–164. https://doi.org/10.21041/ra.v10i2.477.

[55] B. Bhattacharjee, Some issues related to service life of concrete structures, Indian Concr. J. (2012) 23–29.

[56] D. Trejo, R.G. Pillai, Accelerated chloride threshold testing: Part I - ASTM A 615 and A 706 reinforcement, ACI Mater. J. 100 (2003) 519–527.

[57] C. Andrade, Propagation of reinforcement corrosion: principles, testing and modelling, Mater. Struct. Constr. 52 (2019) 1–26. https://doi.org/10.1617/s11527-018-1301-1.

[58] D.K. Kamde, R.G. Pillai, Effect of sunlight/ultraviolet exposure on the corrosion of fusion bonded-epoxy (FBE) coated steel rebars in concrete, Corros. 76 (2020) 843–860. https://doi.org/https://doi.org/10.5006/3588.

[59] D.K. Kamde, M. Zintel, S. Kessler, G.P. Radhakrishna, Performance indicators and specifications for fusion-bonded-epoxy (FBE) coated steel rebars in concrete exposed to chlorides, J. Sustain. Resilient Infrastruct. In press (2020).

[60] D. Darwin, M. O'Reilly, J. Browning, C.E. Locke, Y.P. Virmani, J. Ji, L. Gong, G. Guo, J. Draper, L. Xing, Multiple Corrosion-Protection Systems for Reinforced-Concrete Bridge Components: Laboratory Tests, J. Mater. Civ. Eng. 26 (2014) 1–9. https://doi.org/10.1061/(ASCE)MT.1943-5533.0000991.

[61] D. Trejo, Personal discussion with Prof. David Trejo, Oregon State University, 2020.

[62] U.M. Angst, M.R. Geiker, A. Michel, C. Gehlen, H. Wong, O.B. Isgor, B. Elsener, C.M. Hansson, H. Rob, P. Maria, C. Alonso, M. Criado, M. Sanchez, M. Joa, The steel – concrete interface, Mater. Struct. 50 (2017). https://doi.org/10.1617/s11527-017-1010-1.

[63] D.K. Kamde, R.G. Pillai, Effect of surface preparation on corrosion of steel rebars coated with cement-polymer-composites (CPC) and embedded in concrete, Constr. Build. Mater. 237 (2020) 1–11. https://doi.org/10.1016/j.conbuildmat.2019.117616.

[64] D. Kamde, Electrochemical, bond, and service life parameters of coated steel - cementitious systems exposed to chlorides, Ph.D. Thesis, Indian Institute of Technology Madras, 2020.

[65] J. Karuppanasamy, R.G. Pillai, A short-term test method to determine the chloride threshold of steel – cementitious systems with corrosion inhibiting admixtures, Mater. Struct. 50 (2017) 1–17. https://doi.org/10.1617/s11527-017-1071-1.

[66] A. Schütz, W. Schultz, Moisture absorption and the influence of moisture on the dielectric properties of glass fiber reinforced plastics, Arch. f. Electr. Eng. 77 (1994) 433–440.

[67] SHRP-S-330, Standard Test Method for Chloride Content in Concrete Using the Specific Ion Probe, (1993) 1–118.

[68] S. Rengaraju, Electrochemical Response and Chloride Threshold of Steel in Highly Resistive Concrete Systems, Indian Institute of Technology Madras, 2019.

[69] J.A. Pincheira, A. Aramayo, D. Fratta, K.-S. Kim, Corrosion Performance of Epoxy-Coated Bars in Four Bridge Decks Subjected to Deicing Salts: 30-Year Perspective, J. Perform. Constr. Facil. 29 (2015) 04014097. https://doi.org/10.1061/(ASCE)CF.1943-5509.0000592.

[70] S. Kessler, K. Lau, W.F. Street, A.A. Sagüés, Extent of Cathodic Reaction on Epoxy

Coated Rebar with Partially Disbonded Coating, in: NACE Corros. Conf. Expo, NACE International, Houston, Texas, 2017: pp. 1–12.

[71] K.W.J. Treadaway, H. Davies, Performance of fusion-bonded epoxy-coated steel reinforcement, Struct. Eng. London. 67 (1989) 99–108.

[72] A.B. Darwin, J.D. Scantlebury, Retarding of corrosion processes on reinforcement bar in concrete with an FBE coating, Cem. Concr. Compos. 24 (2002) 73–78.

[73] J.A. González, A. Molina, M.L. Escudero, C. Andrade, Errors in the electrochemical evaluation of very small corrosion rates-I. polarization resistance method applied to corrosion of steel in concrete, Corros. Sci. 25 (1985) 917–930. http://www.scopus.com/inward/record.url?eid=2-s2.0-0021979640&partnerID=40&md5=b7e4720857c16c0e265f59dcee9af2fd.

[74] X.H. Wang, B. Chen, Y. Gao, J. Wang, L. Gao, Influence of external loading and loading type on corrosion behavior of RC beams with epoxy-coated reinforcements, Constr. Build. Mater. 93 (2015) 746–765. https://doi.org/10.1016/j.conbuildmat.2015.05.101.

[75] A.A. Sagues, Technical Note: Equivalent Circuits Representing the Impedance of a Corroding Interface., Corrosion. 44 (1988) 555–557. https://doi.org/10.5006/1.3583975.

[76] J. Song, L. Wang, A. Zibart, C. Koch, Corrosion protection of electrically conductive surfaces, Metals (Basel). 2 (2012) 450–477. https://doi.org/10.3390/met2040450.

[77] A.A. Javidparvar, B. Ramezanzadeh, E. Ghasemi, Effects of surface morphology and treatment of iron oxide nanoparticles on the mechanical properties of an epoxy coating, Prog. Org. Coatings. 90 (2016) 10–20. https://doi.org/10.1016/j.porgcoat.2015.09.018.

[78] K. Kobayashi, K. Takewaka, Experimental studies on epoxy coated reinforcing steel for corrosion protection, Int. J. Cem. Compos. Light. Concr. 6 (1984) 99–116. https://doi.org/10.1016/0262-5075(84)90039-3.

[79] G.G. Miller, J.L. Kepler, D. Darwin, Effect of epoxy coating thickness on bond strength

of reinforcing bars, ACI Struct. J. 100 (2003) 314–320. https://doi.org/10.14359/12606.

[80] IS 13620, IS 13620: FUSION BONDED EPOXY COATED REINFORCING BARS-SPECIFICATION, Bur. Indian Stand. 1993 (2015).